CELL & DEVELOPMENTAL BIOLOGY IN THE DIGESTIVE SYSTEM

Spatial heterogeneity in the mammalian liver

Shani Ben-Moshe and Shalev Itzkovitz *

Abstract | Hepatocytes operate in highly structured repeating anatomical units termed liver lobules. Blood flow along the lobule radial axis creates gradients of oxygen, nutrients and hormones, which, together with morphogenetic fields, give rise to a highly variable microenvironment. In line with this spatial variability, key liver functions are expressed non-uniformly across the lobules, a phenomenon termed zonation. Technologies based on single-cell transcriptomics have constructed a global spatial map of hepatocyte gene expression in mice revealing that ~50% of hepatocyte genes are expressed in a zonated manner. This broad spatial heterogeneity suggests that hepatocytes in different lobule zones might have not only different gene expression profiles but also distinct epigenetic features, regenerative capacities, susceptibilities to damage and other functional aspects. Here, we present genomic approaches for studying liver zonation, describe the principles of liver zonation and discuss the intrinsic and extrinsic factors that dictate zonation patterns. We also explore the challenges and solutions for obtaining zonation maps of liver non-parenchymal cells. These approaches facilitate global characterization of liver function with high spatial resolution along physiological and pathological timescales.

The liver is a multi-tasking organ, performing diverse functions that are critical for maintaining physiological homeostasis. Receiving blood that drains from the intestine, it dynamically controls the metabolite content of the body by storing nutrients absorbed after a meal and releasing them in a regulated manner between meals. In its role as the glucostat of the body[1], the liver is instrumental in maintaining constant blood glucose levels throughout the day — during fasting periods, the organ releases glucose to facilitate systemic glucose requirements but can rapidly shut down release and switch to glucose storage upon feeding. In addition, the liver performs elaborate detoxification processes, forming a crucial line of defence against pathogens and xenobiotics, and has exocrine functions in bile acid production and endocrine functions in the release of hormones. The liver is also one of the main protein synthesis sites in the body, producing a major proportion of the circulating proteins in the blood, including albumin, complement system proteins and blood clotting factors[2].

These diverse liver functions are mostly performed by hepatocytes, the parenchymal cells that constitute 80% of the liver mass and 60% of its cell composition[3]. Liver non-parenchymal cells (NPCs), namely, liver endothelial cells (LECs), hepatic stellate cells, biliary epithelial cells (cholangiocytes), Kupffer cells and additional immune cell populations, support hepatocyte function. Importantly, the liver is not a uniform mass of cells that performs all the above functions equally. Rather, most liver tasks are non-homogeneously carried out by different subsets of hepatocytes, a division of labour that is linked to the anatomical structure of the liver. This division of labour represents a fascinating example of evolutionary optimization of function.

The liver consists of repeating anatomical units termed liver lobules[4] (FIG. 1). The lobules are hexagonal shaped columns measuring ~0.5 mm in diameter in mice and ~1 mm in humans[5]. Blood enters the lobules from the corners, termed the portal nodes, and flows radially inward towards a draining central vein through sinusoidal blood vessels. Hepatocytes are arranged in plates spanning the radial lobule axis. These plates comprise 12–15 hepatocyte concentric layers in mice (FIG. 1). Bile canaliculi transport bile acids secreted by the hepatocytes outwards, in the opposite direction to blood flow, into bile ductules at the portal nodes, from which they are shuttled to the intestine (FIG. 1).

As a result of the polarized blood flow across the lobule, the consumption and secretion of factors by the upstream periportal hepatocytes shape the concentration gradients of these factors (FIG. 1). Thus, the function of periportal hepatocytes modulates the microenvironment sensed by the downstream pericentral hepatocytes. An example is the oxygen concentration across the lobule.

Department of Molecular Cell Biology, Weizmann Institute of Science, Rehovot, Israel.

**e-mail: shalev.itzkovitz@weizmann.ac.il*

https://doi.org/10.1038/s41575-019-0134-x

Key points

- Hepatocytes residing along the lobule porto-central axis are exposed to different microenvironments, resulting in spatial zonation of liver tasks.
- Single-cell technologies have enabled the reconstruction of zonation patterns for the global hepatocyte transcriptome, revealing principles of liver tissue organization.
- Examples of optimal features of hepatocyte zonation include the assignment of energetically demanding tasks to highly oxygenated zones, spatial recycling of material and production line patterns.
- Sequencing pairs of hepatocytes and adjacent non-parenchymal cells enables reconstruction of global zonation patterns of other liver cell types.
- Liver zonation can give rise to zonated patterns of liver pathologies.
- Zonation of gene expression is a prominent feature in other metabolic organs such as the intestine and the kidney.

Approximately 75% of the afferent lobule blood is venous blood that drains from the intestine, with only 25% of the perfusion originating from highly oxygenated arterial blood[6]. Thus, oxygen can be a limiting factor for hepatocytes. As blood flows inwards towards the central vein, hepatocytes respire, and oxygen concentrations decrease. Hepatocytes require oxygen to generate the ATP needed for their many energetically demanding tasks. Particularly costly tasks include the continuous translation of secreted proteins and the process of gluconeogenesis by which hepatocytes generate glucose for secretion in the fasted state. Interestingly, periportal hepatocytes seem to limit their respiration, thus preventing hypoxia of the pericentral hepatocytes[7]. Sinusoidal oxygen tension decreases from 65 mmHg at the portal layers to 30 mmHg in pericentral layers[8]. Considering the additional drop of 10–20 mmHg from the sinusoids to the hepatocytes, pericentral hepatocytes approach but remain safely above hypoxia levels of ~2 mmHg (REF.[9]). Pathological conditions that increase hepatocyte oxygen consumption, such as increased alcohol consumption, lead to pericentral hypoxia[10]. Thus, it seems that hepatocyte respiration is spatially fine-tuned to ensure maximal energy yield for periportal hepatocytes while minimizing risk to pericentral hepatocytes.

Hepatocyte respiration[11] is one example of many liver functions that are non-uniformly distributed along the lobule radial axis, a phenomenon that has been termed liver zonation. The topic of liver zonation has been reviewed elsewhere in excellent publications[2,3,12–15]. In this Review, we briefly describe some of the landmark studies that identified and characterized liver zonation. We then highlight spatial transcriptomics approaches to characterize zonation of all liver genes, review emerging design principles of zonation and discuss the implications of zonation in liver disease.

Metabolic zonation in the liver

Observations of spatial heterogeneity in hepatocytes were reported as early as the beginning of the 20th century. Kater[16] identified graded depositions of glycogen and fat, as well as changes in mitochondria morphology across the porto-central axis of the liver lobule in several model animals. In a cytological study of the mouse liver, Deane[17] found that periportal hepatocytes contain larger mitochondria and have heavier Golgi content, higher concentrations of bile granules, more deposition of glycogen and less deposition of fat than pericentral hepatocytes. She termed this phenomenon 'zonation within the lobule' and attributed it to the graded oxygen and nutrients supplied to the different lobule zones. Chiquoine[18] identified a higher abundance of glucose-6-phosphatase in the periportal zone than in the pericentral zone. Jungermann and colleagues systematically investigated liver zonation in a series of seminal studies[1,19–23]. They proposed the concept of metabolic zonation, whereby gluconeogenesis is carried out by periportal hepatocytes and glycolysis is performed by pericentral ones. Their studies established the functional division of labour of hepatocytes in diverse liver tasks, including periportal oxidative metabolism, gluconeogenesis, ureagenesis, β-oxidation of fatty acids, amino acid breakdown and cholesterol biosynthesis, and pericentral glycolysis, lipogenesis and alcohol detoxification[23] (FIG. 1).

The early studies on liver zonation utilized histochemistry, immunohistochemistry and in situ hybridization (ISH). Although these methods enabled qualitative (and in some cases quantitative) measurements of lobule features in the intact tissue, providing high spatial resolution, they were limited in sensitivity and specificity. For example, the zonation patterns of albumin and other plasma proteins remained inconclusive[24]. The digitonin–collagenase perfusion method emerged as an alternative approach that enabled the isolation of massive amounts of cells enriched for periportal or pericentral hepatocytes[25–28]. In this method, the detergent digitonin is perfused to the liver in either an orthograde or a retrograde direction to selectively damage periportal or pericentral hepatocytes, respectively. This process ensures the enrichment of undamaged cells in the desired zone of interest, which can then be dissociated using collagenase. This technique validated some of the earlier findings that were based on immunohistochemistry and revealed new zonated features, such as the periportal enrichment of albumin mRNA[29]. However, upscaling this approach to whole-transcriptome measurement techniques was required to obtain a global picture of liver zonation.

Whole-transcriptome view of liver zonation

Braeuning et al. generated the first global view of liver zonation[30]. They used digitonin–collagenase perfusion to isolate periportally and pericentrally enriched mouse hepatocytes and measured the whole transcriptome signature of these two populations using microarrays. The high throughput and the increased sensitivity of this approach refined the previous findings on metabolic zonation and uncovered zonation of hundreds of hepatocyte genes.

Using laser-capture microdissection (LCM) to isolate pericentral and periportal hepatocytes followed by microarray measurements, Saito and colleagues also identified hundreds of genes differentially expressed between periportal and pericentral mouse hepatocytes[31]. As with the digitonin–collagenase perfusion method, spatial resolution using LCM was limited to two zones owing to the difficulty in precisely defining multiple lobule layers in tissue sections. In addition, experimental noise and batch effects limit the sensitivity

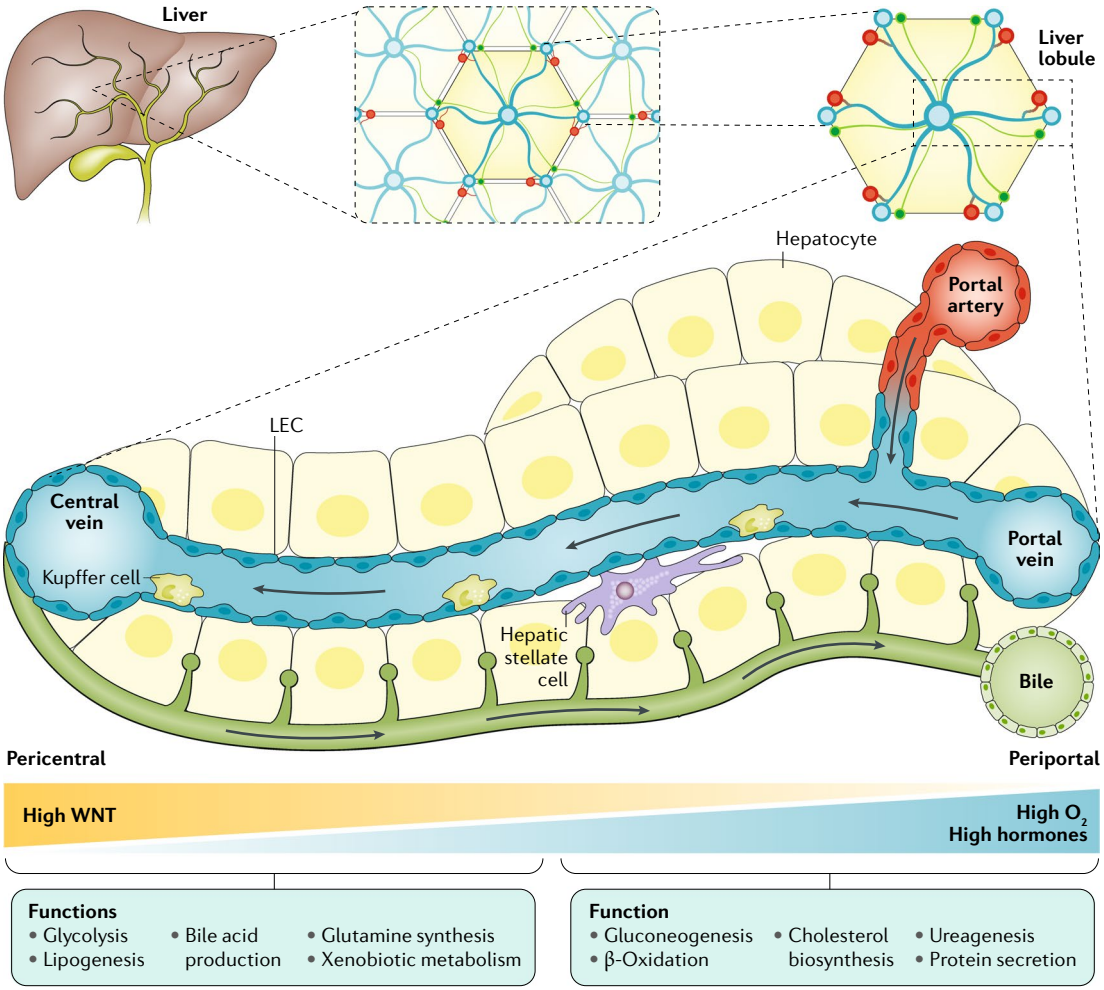

Fig. 1 | **Division of labour in the liver lobule.** The liver is composed of hexagonal lobules. Portal triads consisting of a hepatic artery (red), a portal vein (blue) and bile duct (green) are located at the lobule corners, also termed portal nodes. Blood flows through radial sinusoids and drains into the central vein. Concentric layers of hepatocytes are positioned on the axis between the central vein and the portal node. Liver non-parenchymal cells that support hepatocyte function, such as Kupffer cells (light green), liver endothelial cells (LECs; blue and red) and hepatic stellate cells (purple) reside along the lobule axis. Bile secreted from hepatocytes flows from the central to the portal zone through bile canaliculi that drain into the bile duct. Blood flow and secreted morphogens give rise to a spatially graded microenvironment, resulting in different functions assigned to different layers.

of microarray-based transcriptome measurements. A transcriptome-wide zonation map with higher spatial resolution thus requires other approaches.

Single-cell spatial transcriptomics

Single-cell RNA sequencing (scRNAseq) has emerged as a powerful technology to characterize the complete transcriptomes of cells on a massive scale[32–37]. The technology has several variants but usually entails dissociation of a tissue into single cells, cell lysis and mRNA capture by poly-dT primers that contain a cell barcode, which is a nucleotide sequence that enables mapping of each mRNA molecule back to its original cell. Following RNA capture, reverse transcription and amplification, molecules from thousands of cells are pooled and sequenced using next generation sequencing technology. The reads are then mapped back to the original cells using the cell barcode, yielding the complete transcriptome for thousands of cells in a single experiment. The precision of scRNAseq is enhanced by the use of unique molecular identifiers that label individual mRNA molecules before they are reverse transcribed and amplified, thus preventing amplification biases and enabling the original number of individual mRNA molecules to be estimated[38–41]. The ability to simultaneously sequence thousands of cells and computationally cluster them into coherent cell populations makes up for the low capture rate of transcripts per cell (1–10%[37,42,43]).

scRNAseq requires the dissociation of tissues into isolated cells, resulting in the complete loss of spatial information. To identify spatial patterns of gene expression, the original tissue coordinates of the sequenced cells need to be resolved. Assignment of cells to their original tissue location can be performed on the basis of a subset of landmark genes, for which spatial expression patterns have already been characterized using other approaches. Pioneering studies from the Marioni and Regev laboratories used this approach to reconstruct

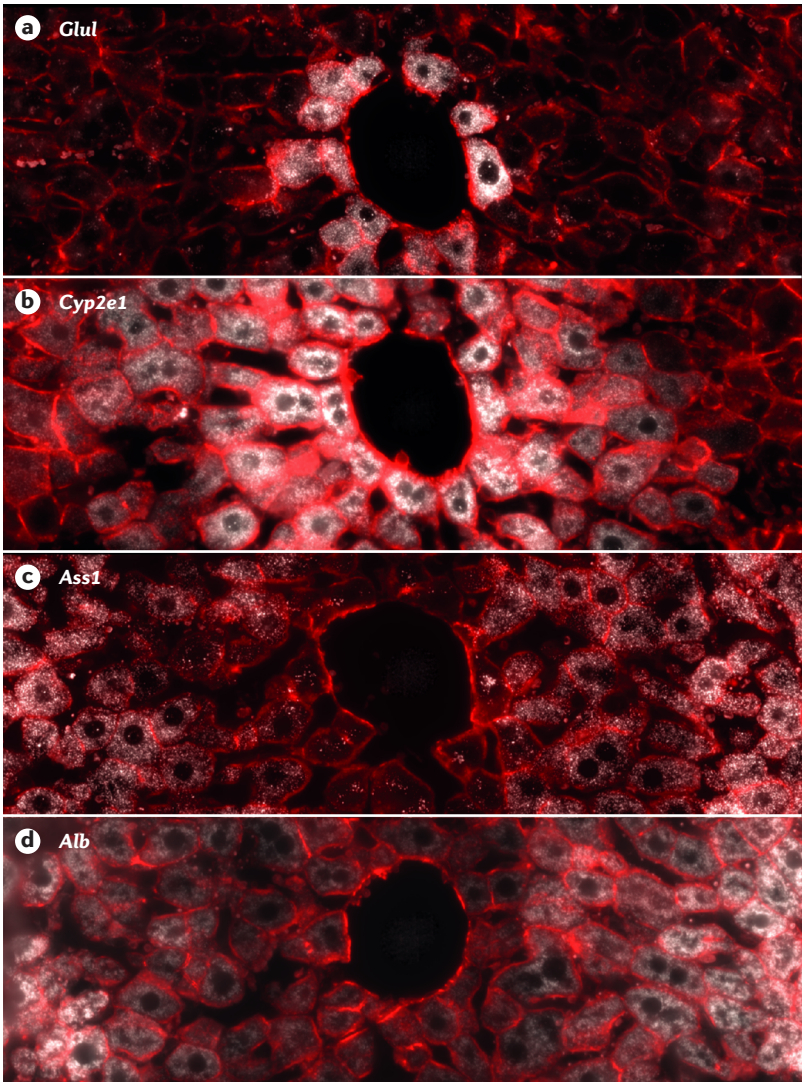

Fig. 2 | **Zonation profiles of landmark genes using single-molecule fluorescence in situ hybridization.** The zonation of two pericentral genes, *Glul* (part **a**) and *Cyp2e1* (part **b**), and two periportal genes, *Ass1* (part **c**) and *Alb* (part **d**), in mouse liver is revealed by single-molecule fluorescence in situ hybridization. White dots are individual transcripts, and hepatocyte membranes are stained red with phalloidin. Precise quantification of the zonation profiles of these and other landmark genes, together with single-cell RNA sequencing of hepatocytes, facilitates global reconstruction of hepatocyte zonation[48]. Parts **a**–**d** reproduced from REF.[48], Springer Nature Limited.

spatial gene expression maps of embryos[44,45]. These studies required a large landmark gene panel of dozens of genes, which was obtained using traditional ISH. Although ISH and immunofluorescence have been applied in the liver, these techniques are limited in sensitivity and dynamic range[46]. The accurate spatial mapping of dissociated single hepatocytes requires more precise quantitative methods to characterize landmark genes.

Single-molecule fluorescence ISH (smFISH) is an alternative to traditional ISH that enables measuring the absolute numbers of mRNA molecules in cells in situ[47]. This approach entails hybridizing tissue sections with multiple singly labelled fluorescent probes designed to be complementary to sequential parts of the mRNA of interest. The local accumulation of these multiple probes on single transcripts reveals them as bright spots under a fluorescence microscope. These dots are counted to yield a precise gene expression signature for selected landmark genes in distinct lobule zones. Bahar Halpern et al. used smFISH to map the zonation profiles of a small set of six landmark genes in mouse liver sections — the pericentrally zonated genes *Glul* and *Cyp2e1* and the periportally zonated genes *Ass1*, *Asl*, *Alb* and *Cyp2f2* (REF.[48]) (FIG. 2). These genes were chosen on the basis of previously identified zonation patterns and their high expression levels (BOX 1). The selection of landmark genes with high expression levels ensured that each of the sequenced hepatocytes would include molecules from these six landmark genes even with the low capture rate of 1–10% of the cellular transcripts that is typical of scRNAseq. Additional considerations for the choice of landmark gene sets are described in BOX 1.

The ability of smFISH to resolve intermediate expression levels enabled the reconstruction of zonation maps for these six landmark genes over nine concentric layers spanning the porto-central axis (FIG. 3). Next, Bahar Halpern et al. performed scRNAseq of hepatocytes, extracted by perfusing mouse livers, and developed a computational algorithm to infer the original lobule layer of each of the sequenced cells on the basis of the scRNAseq expression of the six landmark genes[48]. For each gene, expression was then averaged over the hundreds of cells assigned to each of the nine lobule layers to produce zonation profiles for all hepatocyte genes (FIG. 3). The predicted zonation profiles were comprehensively validated by smFISH, establishing the accuracy of this technique. This approach therefore enabled the generation of a global expression map of liver zonation with high spatial resolution[48].

Principles of liver zonation

The studies on hepatocyte zonation suggest several principles of liver tissue organization (FIG. 4).

Scope and patterns of liver zonation. Approximately half the genes expressed in mouse hepatocytes are zonated (~3,500 genes out of 7,000 are differentially expressed along the lobule)[48]. With a few exceptions, zonation of most genes is not binary but rather consists of gradients of expression, often with a dynamic range of less than twofold (FIG. 4a). Thus, the spatial division of labour among hepatocytes seems to be a fuzzy assignment task, in which different hepatocytes distribute their available resources between many tasks in a spatially graded manner.

Zonation of energetically demanding tasks. Energetically demanding tasks, such as protein secretion and gluconeogenesis, are preferentially assigned to the highly oxygenated periportal lobule layers, where hepatocytes can more readily generate ATP through respiration (FIG. 4b). Such periportally zonated hepatocyte genes include the genes that encode secreted proteins such as albumin, complement system proteins and blood clotting factors. Indeed, protein translation, which is required for massive secretion, is one of the most ATP-demanding tasks for cells[49]. Gluconeogenesis is another energy-consuming hepatocyte task, requiring

more than 15% of liver ATP in a fasted state[50], and its periportal predominance is evidenced by the expression of the *Pck1* gene, which encodes the gluconeogenic enzyme phosphoenolpyruvate carboxykinase 1 (REFS[48,51]).

Mid-lobule hepatocyte tasks. Previous studies of liver zonation considered the mid-lobule layers, traditionally termed zone 2 (REF.[52]), to be a transition zone between periportal and pericentral zones. By contrast, the spatial

Box 1 | **Considerations for choosing landmark genes**

Spatial reconstruction of single cells is based on the premise that the mRNA numbers of landmark genes can be used as molecular barcodes to derive information on cellular location. The success of this approach depends on the choice of the landmark gene panel. Here, we highlight some important considerations when choosing landmark genes:

a | Spatial resolution

The landmark gene panel should provide information on the entire spatial unit that is interrogated. Consider spatial reconstruction of hepatocytes over a lobule that is sub-divided into nine concentric layers on the basis of the expression of a single landmark gene (*LM*). The gene in the top panel is highly abundant in pericentral layer 1 and has expression that is close to 0 in layers 4–9. Hepatocytes classified on the basis of the single-cell expression values of this gene would probably be correctly placed into layers 1–3, yet there is not enough information to correctly place cells within layers 4–9. The gene in the bottom panel, on the other hand, is also expressed pericentrally, yet expression decreases gradually from layer 1 to layer 9. The expression levels of this gene therefore provide more spatial information. Hepatocytes with high expression are most likely to originate from layer 1, whereas hepatocytes with intermediate expression levels are likely to derive from layers 4–5, and hepatocytes with very low expression levels probably come from layer 9.

b | Number of landmark genes

Using multiple landmark genes provides more information on location than using a single landmark gene. Spatial information can be gained by using both sharply zonated genes that peak in different lobule layers and genes that are gradually zonated. Including more than one landmark gene can assist in determining the likelihood of cell positioning when landmark gene expression values are ambiguous. In this example, a cell from layer 5 may be incorrectly assigned to layer 6 on the basis of *LM1* expression level (top) and to layer 4 on the basis of *LM2* expression level (bottom). When combining the information from both landmark genes, the cell location is correctly inferred.

c | Intra-layer variability

An optimal landmark gene should have low variability in single cells from the same zone to minimize layer misclassification. In the example shown in the bottom panel, the cell could be misplaced in layer 4 instead of layer 6, as the expression of this landmark gene is highly variable. In likelihood-based algorithms, genes that display high variability can be assigned less weight[48].

d | Expression levels

Single-cell RNA sequencing (scRNAseq) captures ~1–10% of the transcripts in a cell. This low yield poses a limit on the ability to correctly classify cells. Sampling is a Poisson process that yields a standard deviation of mRNA counts that equals the square root of the mean[190]. Consequently, the relative standard deviation (standard deviation divided by the mean) increases as the mean decreases. Therefore, the lower the mRNA transcript counts, the noisier the data. As an example, consider a gene expressed at 100 copies per cell in periportal hepatocytes and 50 copies per cell in pericentral hepatocytes (top panel). If the porto-central radial lobule coordinate is the only factor that shapes gene expression, then the mRNA counts in these cells would be Poisson-distributed (100 ± 10 versus ~50 ± 7). Obtaining the full counts of mRNA molecules per cell for this gene should make it quite straightforward to classify them. However, if a sample of only 10% of the transcripts in these cells is taken (bottom panel), the expression levels would now be ~10 ± 3 copies for periportal hepatocytes and ~5.0 ± 2.5 copies for pericentral hepatocytes. Importantly, although the average number of mRNA copies per cell decreased by tenfold, the standard deviation scales as the square root of the mean and therefore decreases less. It would now be quite common to misclassify the spatial location of the cells on the basis of this landmark gene. Thus, using highly expressed landmark genes increases the statistical power to identify cellular location. Alternatively, using more landmark genes can also reduce the uncertainty in classification.

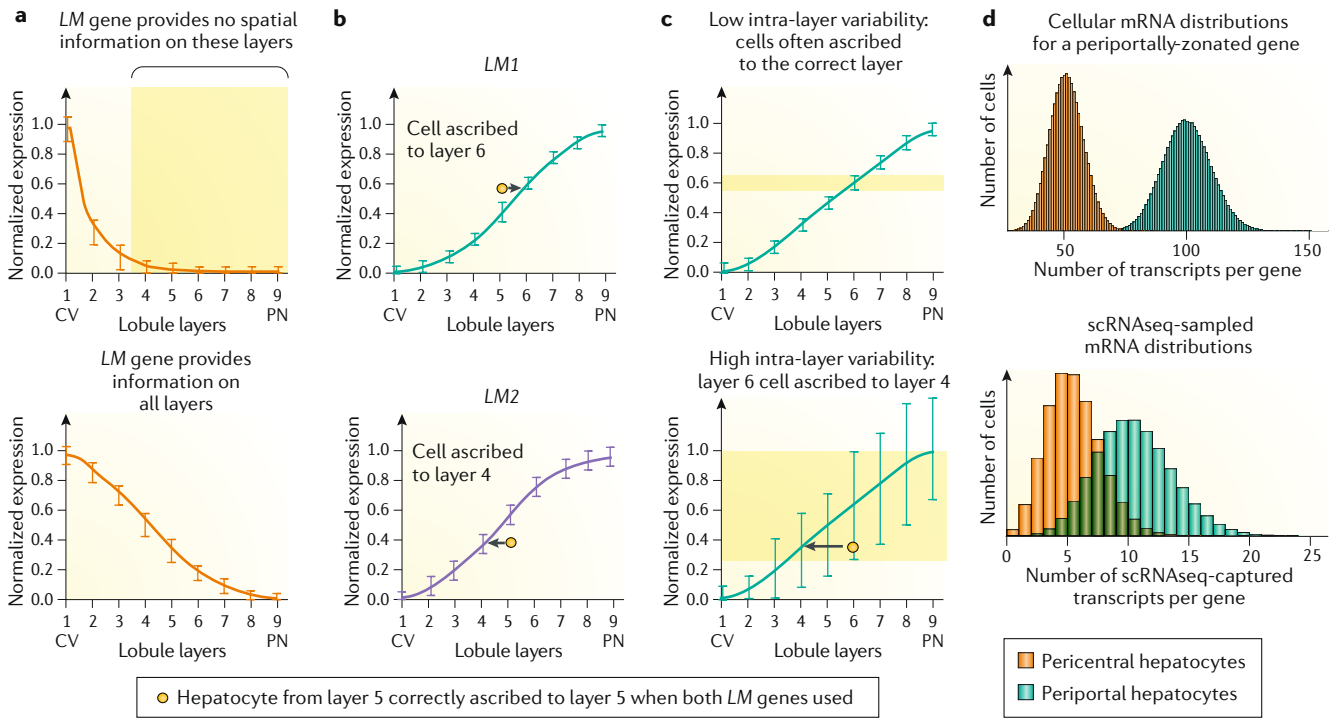

CV, central vein; PN, portal node.

transcriptomics reconstruction[48] revealed that several important hepatocyte genes exhibit zonated expression profiles that peak in these mid-lobule layers (FIG. 4c). These genes include *Hamp* and *Hamp2* (REF.[53]), which encode the hepcidin hormone that regulates systemic iron levels. Additional examples include *Igfbp2*, encoding the protein IGFBP2 that binds insulin growth factors and modulates their binding properties. Thus, the

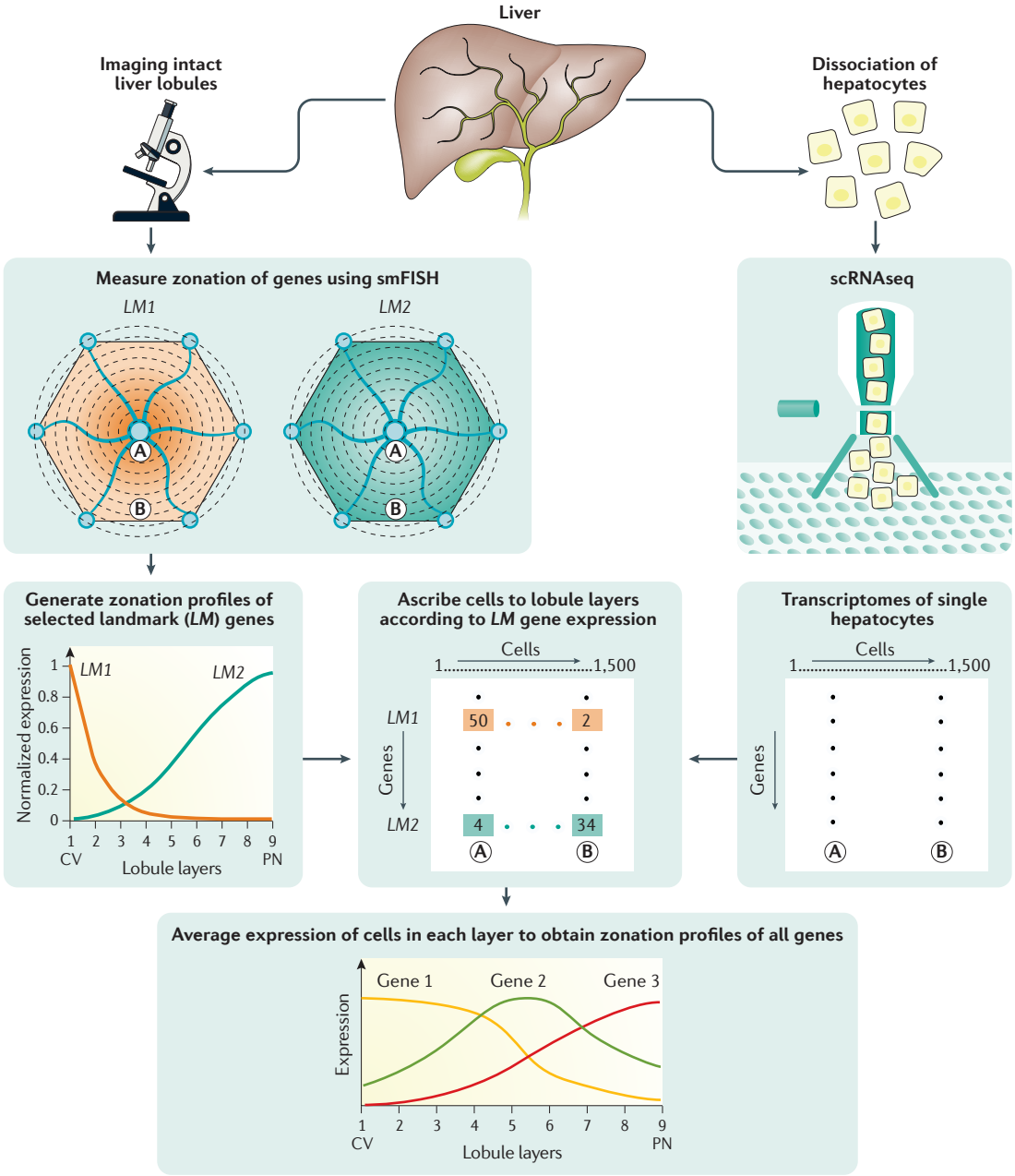

Fig. 3 | **Single-cell spatial reconstruction of hepatocyte transcriptomes using landmark genes.** This strategy has been used to obtain the zonated pattern of all hepatocyte genes[48]. Single-molecule fluorescence in situ hybridization (smFISH) is used to reveal mRNA expression levels in the intact tissue, enabling the zonation patterns of landmark genes (*LM*) to be measured with a high spatial resolution. Next, the liver is dissociated into single hepatocytes that undergo single-cell RNA sequencing (scRNAseq), revealing the complete transcriptome of thousands of hepatocytes. scRNAseq provides high-throughput expression levels for all genes but does not capture spatial information. The original lobule layer of each sequenced hepatocyte is inferred on the basis of the expression levels of the landmark genes. For example, cell A has high levels of the pericentral *LM1* gene (orange) and low levels of the periportal *LM2* gene (green). Hence, cell A is assigned to pericentral layer 1. Conversely, cell B has low levels of *LM1* and high levels of *LM2* and is therefore assigned to periportal layer 9. Next, the hepatocytes are grouped by their lobule layer of origin, and the mean expression level of each gene in each layer is calculated. This analysis enables zonation patterns for the whole hepatocyte transcriptome to be inferred. Note that lobule layers are enumerated from the most pericentral layer (layer 1, traditionally termed zone 3 (REF.[52])) to the most periportal layer (layer 9, traditionally termed zone 1 (REF.[52])). This enumeration scheme highlights the importance of the central vein as a signalling hub that largely shapes hepatocyte zonation. CV, central vein; PN, portal node. Adapted from REF.[48], Springer Nature Limited.

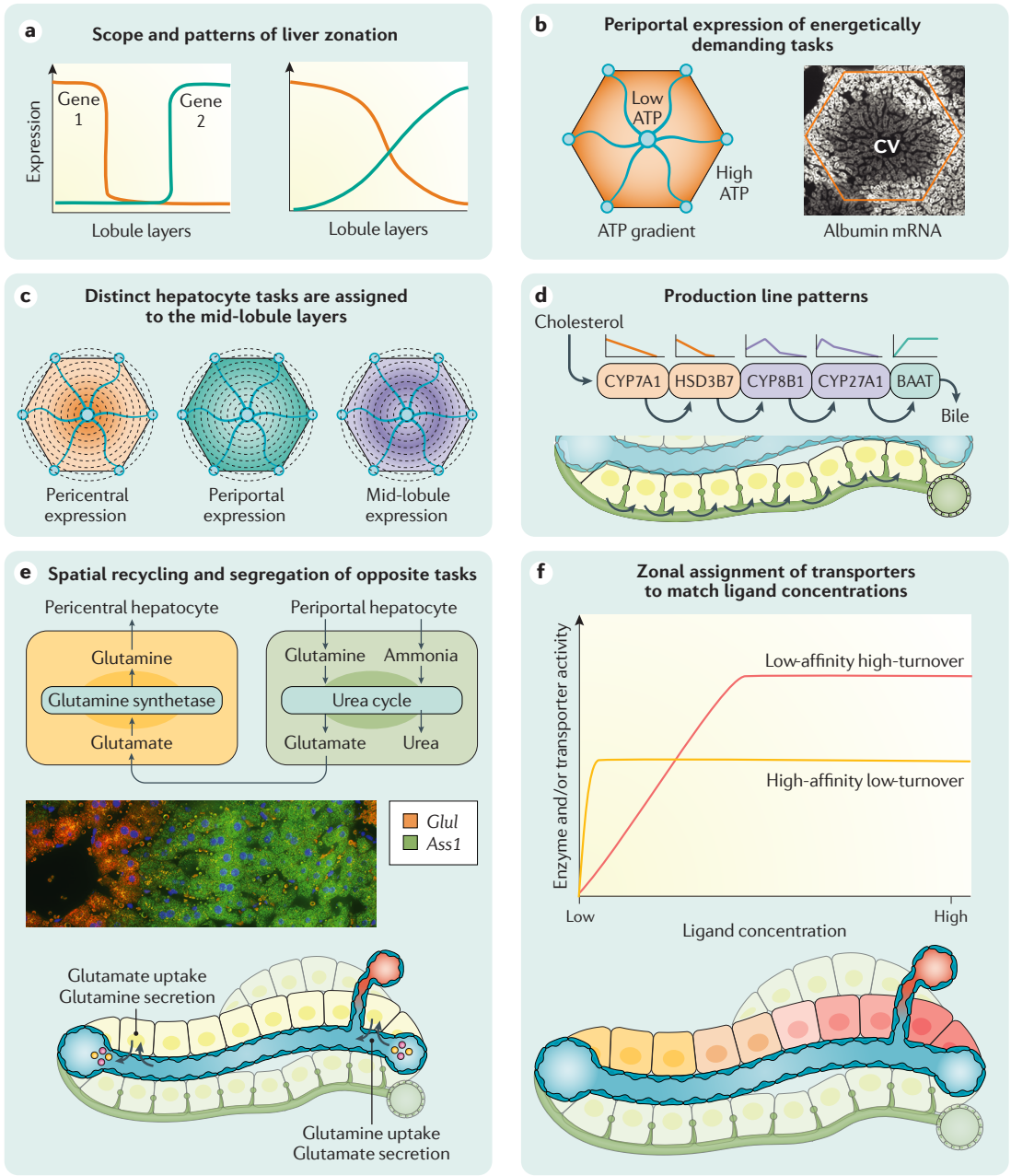

Fig. 4 | **Principles of hepatocyte zonation. a** | Most zonated liver genes have a graded expression pattern across lobule layers rather than binary ON or OFF expression. **b** | Energy-demanding tasks, such as synthesis of secreted proteins including albumin, are assigned to the more highly oxygenated periportal layers, where hepatocytes can obtain a higher ATP yield (left panel). Single-molecule fluorescence in situ hybridization (smFISH) for albumin mRNA shows a periportal zonation pattern (right panel). **c** | Specific hepatocyte tasks are enriched in the mid-lobule layers, for example, expression of *Hamp*, which encodes the iron regulator hormone hepcidin. **d** | Sequential enzymes in a metabolic pathway are expressed in sequential lobule layers. This production line pattern could indicate that metabolite intermediates are transferred from one hepatocyte layer to the next. One such example is the neutral bile acid biosynthesis pathway, in which sequential enzymes peak in expression in sequential layers in line with the central–portal bile acid secretion direction. **e** | Spatial recycling and segregation of opposing tasks. In the glutamine–glutamate homeostasis example shown, periportal hepatocytes take up glutamine and ammonia and excrete urea and glutamate (green box), whereas the most pericentral hepatocytes recycle the glutamate back to glutamine (orange box). The smFISH image shows the distribution of *Ass1* mRNA (green), which encodes argininosuccinate synthase, a key enzyme in the urea cycle, and *Glul* mRNA (orange), encoding glutamine synthetase in the most pericentral layer. **f** | The properties of enzymes and transporters expressed along the liver lobule are matched to ligand concentrations. Transporters or enzymes with high turnover rates yet low affinities (red) are assigned to periportal layers, where input ligand concentrations are higher. Transporters or enzymes with high affinity and low turnover rates (yellow) are assigned to pericentral layers, in which the ligand concentrations have already been reduced owing to their uptake by upstream periportal hepatocytes. In an example of this zonation pattern, GLUT1, a high-affinity transporter for glucose, is expressed pericentrally, whereas GLUT2, which has high turnover and low glucose affinity, is expressed periportally. CV, central vein; PN, portal node. Part **e** reproduced from REF.[48], Springer Nature Limited.

mid-lobule layers are not simple transition zones but rather have prescribed functions.

Production line patterns. The high spatial resolution of the liver zonation map[48] revealed examples of spatially distributed metabolic cascades. In these examples, sequential enzymes in a metabolic cascade are expressed in sequential lobule layers, hinting at potential production line patterns in which intermediate metabolites might be transferred from one cell layer to the next (FIG. 4d). An example of this process is the neutral bile acid biosynthesis cascade. One of the main hepatocyte tasks is the production of bile acids[2], which are secreted into the bile canaliculi and drained into the intestine, where they assist in lipid absorption. The pericentrally localized neutral bile acid biosynthesis cascade consists of uptake of cholesterol from the blood and its conversion into bile acids, either cholic acid or chenodeoxycholic acid (CDCA)[54,55], through a series of enzymatic steps. Interestingly, although the first two enzymes in the cholic acid production cascade, CYP7A1 and HSD3B7, are expressed at the highest levels in layer 1 (the most pericentral layer), the next enzyme in the cascade, CYP8B1, is downregulated in layer 1 and has peak expression in layer 2. This pattern could indicate that products of the two first enzymatic steps are transferred, either through gap junctions, the bile canaliculi or the space of Disse, to be taken up by the layer 2 hepatocytes that carry out the next enzymatic step in the cascade[48]. In addition to CYP7A1, the expression of key enzymes, such as CYP3A11, that convert CDCA to muricholic bile acids[56] also peaks at layer 1 (REF.[48]). The zonation profiles of these enzymes might therefore alternatively indicate increased production of CDCA in layer 1 and cholic acid in layer 2. Proving production line hypotheses requires zonation patterns of metabolites to be generated, a challenge described later.

Additional examples of production line patterns include the secretion of insulin growth factors. IGF1 is expressed by periportal hepatocytes and secreted into the sinusoids, whereas IGFBP2, a binding factor of IGF1 that affects its systemic binding properties, is expressed by mid-lobule hepatocytes, downstream along the direction of blood flow[48]. The functional advantages of production line patterns over an alternative strategy of correlated levels of expression of all enzymes in a metabolic cascade by the same hepatocyte remain to be resolved.

Spatial recycling. Liver zonation includes examples of spatial recycling, in which metabolites produced by periportal hepatocytes, such as glucose and glutamate, are taken up by pericentral hepatocytes. As the glucostat of the body, the liver utilizes glucose mainly for storage as glycogen, rather than for cellular energy production, and dynamically shifts between glucose release and uptake. During fasted states, when systemic glucose levels are low, both periportal and pericentral hepatocytes release glucose[19,20]. Following a meal, when blood glucose levels are high, these hepatocytes shift to glucose uptake and rebuild their glycogen stores. Interestingly, at intermediate glucose levels, it has been suggested that periportal hepatocytes release glucose while pericentral hepatocytes uptake glucose[57]. Indeed, expression of *G6pc*, encoding glucose-6-phosphatase, a major enzyme involved in hepatic glucose output, is periportally zonated, whereas expression of *Gck*, encoding the enzyme glucokinase that is essential for detainment of cellular glucose via its phosphorylation, is pericentrally zonated[48,58]. In these intermediate metabolic states, recycling of glucose by pericentral hepatocytes might enable rapid responses to acute reductions in blood glucose concentrations. In these instances, cessation of glucose uptake by pericentral hepatocytes would lead to rapid elevation of the hepatic glucose output, as periportal hepatocytes are already in glucose output mode[57].

A second example of spatial recycling is the periportal expression of *Gls2*, which encodes the enzyme glutaminase 2 that converts glutamine to glutamate, and the pericentral expression of *Glul*, encoding glutamine synthetase, which reconverts glutamate into glutamine. Glutamate breakdown is required for the hepatocyte urea cycle, one of the main hepatocyte tasks[59–63]. The urea cycle is a mechanism to remove ammonia, a toxic molecule that is constantly produced by the body as a result of protein breakdown. By consuming glutamine from the blood, the periportal hepatocytes are able to convert ammonia into urea while generating glutamate as a by-product (FIG. 4e). Both urea and glutamate are released into the sinusoids and accumulate as blood flows pericentrally[59]. However, whereas the kidneys eventually excrete urea, glutamine must be recycled to maintain the amino acid balance of glutamate and glutamine. Indeed, the pericentral layer of hepatocytes specifically expresses glutamine synthetase[61], efficiently converting the accumulated glutamate back to glutamine. The intercellular glutamine cycle has other physiological effects, such as control of blood pH[64].

Spatial segregation of opposing tasks. The liver carries out several antagonistic tasks implemented by catabolic and anabolic enzymes. Examples include the production of glucose by gluconeogenesis and its consumption via glycolysis; the oxidative break down of fatty acids and lipid biosynthesis; the hydrolysis of glutamine to glutamate and the inverse synthesis of glutamine from glutamate; and the production and consumption of cholesterol. Expressing enzymes carrying these opposing processes within the same cell could result in futile cycles[23,63]. Instead, the key enzymes associated with these antagonistic processes seem to be inversely zonated: gluconeogenesis, glutamine breakdown and cholesterol biosynthesis are periportally zonated, whereas glycolysis, glutamine synthesis and cholesterol consumption via bile acid biosynthesis are pericentrally zonated (FIG. 1). β-Oxidation and lipid biosynthesis have also been traditionally considered to be spatially segregated, with β-oxidation being carried out in periportal regions and lipid biosynthesis being performed pericentrally. However, some studies support a periportal predominance of both processes[65].

Zonation of transporters. The consumption and production of nutrients and hormones by hepatocytes along the porto-central lobule axis create gradients of these factors[12]. In pericentral regions, the concentrations of substrates consumed by hepatocytes decrease while the

concentrations of products increase. Many nutrients are substrates for several cellular transporters that differ in their properties, specifically their affinity and maximal transport rate (or turnover number[66]). A high-affinity transporter can facilitate transport of its cognate nutrient into the cell even if the nutrient is found at very low concentrations but could have a lower maximal transport rate when the concentrations of the nutrient are high. Conversely, high-turnover transporters with low affinities would be less efficient in transport of nutrients present at low concentrations (FIG. 4f).

The spatial transcriptomics liver zonation map[48] indicates that the low-affinity high-turnover glucose transporter GLUT2 is predominantly expressed more highly in periportal hepatocytes, whereas the high-affinity low-turnover glucose transporter GLUT1 (REF.[67]) is expressed more highly in pericentral hepatocytes. Periportal GLUT2 expression would facilitate more efficient uptake of glucose during a meal, as periportal glucose concentrations are higher than pericentral glucose concentrations[57]. As blood flows pericentrally, glucose levels decrease owing to hepatocyte uptake, and hepatocytes shift to the expression of GLUT1, which more efficiently transports glucose at low concentrations. The pericentral expression of GLUT1 also ensures a constant slow uptake of glucose in pericentral hepatocytes in all metabolic states, independent of the precise sinusoidal glucose concentrations.

The process of ammonia detoxification described earlier (FIG. 4e) is another example of assignment of processes that match ligand concentrations. In addition to its role in reconverting glutamate to glutamine to counterbalance its periportal breakdown, the pericentral process of glutamine synthesis is also a high-affinity ammonia detoxification mechanism, operating more efficiently than the urea cycle when ammonia concentrations are low[59,64,68]. Consequently, conducting glutamine synthesis pericentrally is optimal for scavenging the remaining ammonia molecules that escaped detoxification from the periportal zones.

Zonation of liver non-parenchymal cells

All liver functions described thus far are carried out by hepatocytes. Although hepatocytes are the main cell type in the liver, ~40% of hepatic cells are NPCs[3]. These cells predominantly include LECs, hepatic stellate cells, cholangiocytes, Kupffer cells and diverse additional immune cell types (FIG. 1). Many of these cell types are static and are thus exposed to the same spatial gradients as the hepatocytes. It is thus important to understand whether they also exhibit spatial functional heterogeneity. LECs make up ~50% of the NPCs. These cells form the blood vessels, clear endotoxins, bacteria and other compounds, regulate host immune responses to pathogens, present antigens and secrete morphogens that shape hepatocyte gene expression[69–72]. Of particular note is the layer of pericentral LECs that produce WNT ligands and RSPO3, key morphogens that shape hepatocyte zonation[73–75].

Spatial reconstruction of LEC gene expression using landmark genes is challenging, as LECs are much smaller than hepatocytes. Whereas hepatocytes contain ~700,000 mRNA molecules[48], a typical LEC contains only ~30,000 mRNA molecules[76]. With the low capture rate of 1–10% of the cellular transcripts associated with scRNAseq[43], each sequenced LEC will therefore contain only several hundred individual transcripts. Because these transcripts are derived from several thousands of genes expressed by these cells, most LEC-expressed genes will have zero reads in any individual sequenced cell. Thus, whereas six highly expressed landmark genes were sufficient for inferring the spatial location of hepatocytes, dozens of LEC landmark genes would be required to facilitate similar spatial reconstructions of LECs.

To overcome this limitation, Bahar Halpern et al. developed an approach termed paired-cell RNA sequencing (pcRNAseq[76]) (FIG. 5). They sub-optimally dissociated liver tissue to yield pairs of cells that were originally attached within the tissue. They next sorted hepatocytes on the basis of size and selected cells that were positive for CD31, an LEC surface marker. The resulting sorted pairs mostly consisted of a single hepatocyte and an attached LEC. The transcriptomes of thousands of such pairs were subsequently sequenced, and each pair of cells could then be localized along the lobule axis on the basis of the expression of hepatocyte genes. Next, genes that were expressed exclusively in LECs were determined from scRNAseq data of hepatocytes and LECs, and the zonation profiles of these LEC genes could be determined from the spatially localized pairs.

The spatial reconstruction indicated that LECs are also highly zonated, with more than 30% of their genes expressed in a spatially heterogeneous manner. The LEC zonation reconstruction exposed the expression signature of the pericentral LECs that, in addition to expressing the WNT signalling ligands *Wnt2*, *Wnt9b* and *Rspo3*, also expressed *Dkk3*, a WNT modulator that is expressed in a subset of pericentral LECs. Thus, the pericentral endothelial niche consists of subpopulations that jointly shape the pericentral morphogenetic fields.

pcRNAseq is a generic approach that can be used to uncover zonation patterns of other liver NPCs. Kupffer cells, the liver-resident macrophages, have critical roles such as phagocytosis of red blood cells and bacterial engulfment. Previous work using immunohistochemistry and digitonin–collagenase perfusion isolation suggested that these NPCs might also be spatially heterogeneous[77]; however, a global zonation map of Kupffer cells has not yet been attained. Such a map could resolve potential sub-specialization of Kupffer cells at different lobule layers. Another natural candidate for spatial reconstruction using pcRNAseq is the hepatic stellate cell, a vitamin A-storing cell that is activated by liver damage, resulting in dramatic phenotypic changes including the secretion of extracellular matrix[78,79]. pcRNAseq could resolve zone-dependent expression patterns and activation of these NPCs in pathological states.

Regulation of hepatocyte zonation

Hepatocyte gene expression is shaped by diverse external inputs, including concentrations of metabolic hormones (such as insulin and glucagon), oxygen, nutrients and morphogens. As these factors are consumed and/or degraded by hepatocytes, they often exhibit gradients

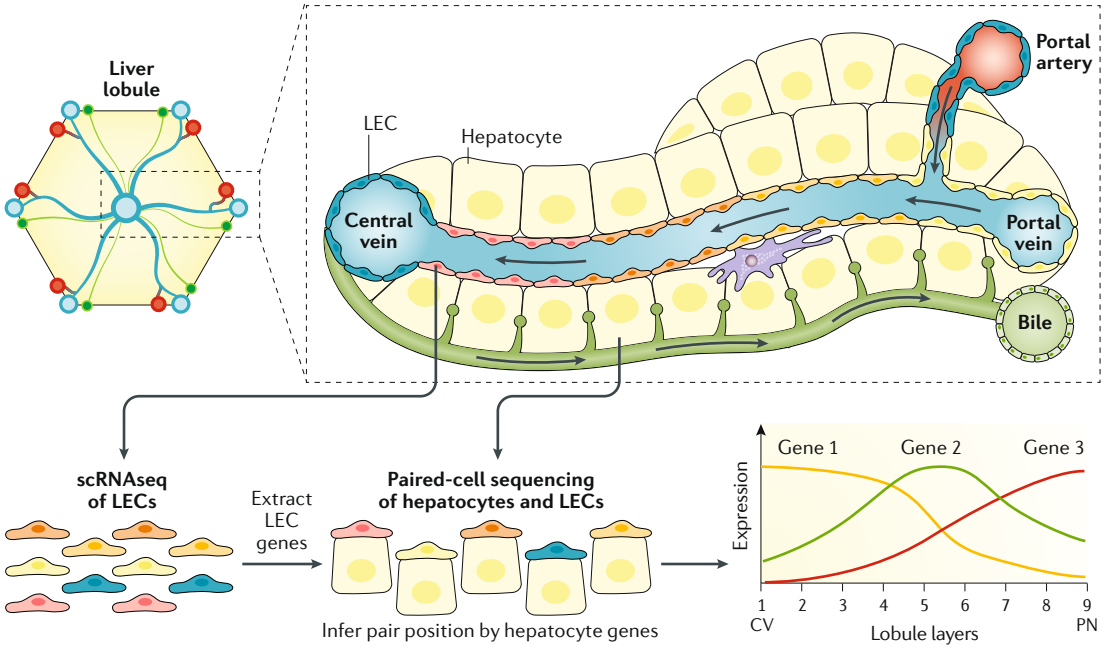

Fig. 5 | **Paired-cell RNA sequencing to infer liver endothelial cell zonation.** In this approach, the liver is partially dissociated, and cell pairs consisting of a hepatocyte and adjacent liver endothelial cell (LEC) are sequenced together. The hepatocyte transcripts are used to localize the pairs of cells along the lobule porto-central axis on the basis of hepatocyte landmark gene expression. Next, single-cell RNA sequencing (scRNAseq) of pure LECs is used to determine which genes are exclusively expressed in LECs and not in hepatocytes. The expression levels of these genes in the localized cell pairs can be used to reconstruct their spatial zonation profiles. CV, central vein; PN, portal node.

of concentrations along the lobule axis, potentially explaining liver zonation patterns.

WNT morphogens are secreted from LECs that line the central vein and diffuse periportally as their levels decrease owing to degradation[73]. These morphogens, particularly WNT2 and WNT9B produced by pericentral LECs[73,76,80], seem to be particularly important for shaping liver zonation[6,15,81,82]. Upon binding of WNT morphogens to hepatocyte receptors, an intracellular signalling cascade elicits stabilization and nuclear translocation of β-catenin, resulting in transcriptional induction and repression of a wide range of target genes[6]. Approximately one-third of the ~3,500 zonated hepatocyte genes are WNT targets and exhibit an expression pattern that is consistent with WNT regulation — WNT-activated genes are mostly pericentrally zonated, whereas WNT-repressed genes are mostly periportally zonated[48]. Mutant mouse models in which hepatic WNT signalling is enhanced exhibit increased expression of pericentral genes in periportal zones and reduced levels of expression of periportal genes, whereas inactivation of the WNT signalling pathway changes pericentral expression patterns into periportal-like expression patterns[80,82–84]. R-spondin is another morphogen produced by pericentral endothelial cells that potentiates WNT signalling and seems to be an important determinant of hepatocyte zonation[74,75,85]. Liver-specific deletion of RSPO3, although not affecting WNT2 and WNT9B levels, resulted in the downregulation of WNT canonical targets — AXIN2 and LGR5, as well as centrally zonated genes such as *Glul*, *Cyp7a1* and *Oat* — and upregulation of periportal genes, such as *Cyp2f2*, *Cdh1* and *Hsd17* (REF.[85]). Similar results were observed in mice with liver-specific double deletion of the R-spondin receptors LGR5 and LGR4 (REF.[75]). Studies published in the past few years have suggested that Hedgehog morphogens might also shape hepatocyte zonation[14,86].

Several studies established the role of oxygen in modulating hepatocyte zonation[8,9,87,88]. Exposing cultured hepatocytes to low oxygen tension induced the expression of pericentral genes, whereas high oxygen tension induced periportal genes[87,88]. Additionally, hypoxia-induced genes are expressed more strongly in the pericentral zones, consistent with the pericentrally decreasing concentration of oxygen[48]. Hypoxia-induced factor 1 (HIF1) is a transcription factor regulating pericentral genes, such as *Slc2a1*, which encodes GLUT1 (REF.[48]). Upon low oxygen availability, HIF1 subunits are stabilized, heterodimerize and translocate into the nucleus, where they bind hypoxia-response elements on target genes[8,89]. HIF1 has also been found to directly interact with β-catenin[90,91], in agreement with pericentral regulation.

The pancreatic hormones glucagon and insulin are important blood-borne factors that shape liver zonation. These antagonistic hormones are differentially degraded by hepatocytes as blood flows pericentrally, yielding a higher ratio of glucagon to insulin in periportal regions than pericentral regions[2]. A study published in 2018 showed that glucagon counteracts β-catenin activity by inducing periportal gene expression and that glucagon knockout mice have reduced expression of periportal genes[92]. Pituitary-dependent signals mediated by growth hormone and thyroid hormone regulate sex-specific liver cytochrome P450 enzymes that hydroxylate steroid hormones, among other substrates[93]. This regulation is evidenced by the periportal induction of the expression

of these enzymes after hypophysectomy in male and female rats[94].

The picture depicted here of hepatocyte zonation regulation by spatially graded extrinsic inputs assumes that all hepatocytes are essentially identical cell types. Under this premise, if a pericentral hepatocyte was transferred to the periportal zone, it would exhibit the same gene expression patterns as the surrounding periportal cells. An alternative hypothesis for liver zonation posits that hepatocytes at different zones might carry different epigenetic features such as DNA methylations or chromosomal conformations. These features change over longer timescales than signals from the local tissue milieu and are often the defining features of a cell type, as they dictate the cellular response to specific inputs[95,96]. Indeed, a study published in 2018 revealed differences in methylation patterns between periportal and pericentral human hepatocytes, which correlated with zonated gene expression[97]. Systematic characterization of the epigenetic features of zonal hepatocytes would lead to a deeper understanding of their zonal identities.

Liver zonation in pathological states

Liver pathologies often exhibit zonated patterns that can be attributed to the functional zonation of hepatocytes. An example is the pericentral damage associated with drug-induced liver injury. The pericentral expression of P450 enzymes results in increased exposure of the expressing hepatocytes to toxic intermediates that accumulate when an input drug is overdosed. CYP2E1 and CYP1A2 are P450 enzymes that convert acetaminophen (also known as paracetamol or APAP) into the toxic intermediate *N*-acetyl-p-benzoquinoneimine (NAPQI), which is in turn converted by glutathione transferases into a stable metabolite that is excreted[98–101]. Consistent with the pericentral zonation of CYP2E1 and CYP1A2, an overdose of APAP gives rise to pericentral damage[101]. Conversely, the anticancer drug doxorubicin can lead to liver damage, predominately in the periportal zones. This zonated hepatotoxicity is attributed to the redox cycling of the drug in the more oxygenated portal zones[102]. Different compounds and xenobiotics can lead to either pericentral or periportal damage. Compounds damaging the pericentral layers include carbon tetrachloride (CCl_4)[103] and ethanol[104], and compounds damaging the periportal layers include galactosamine[105] and allyl alcohol[106] (BOX 2).

Fatty liver disease is a common liver pathology that progresses in a zonated manner. The course of fatty liver disease begins with the accumulation of lipid droplets, causing steatosis, which in turn can lead to cirrhosis and hepatocellular carcinoma (HCC)[107]. The increased expression of lipogenesis genes and reduced expression of fatty acid β-oxidation genes in pericentral hepatocytes (FIG. 1) suggest that lipid accumulation might be faster in this zone than in periportal regions in pathological conditions. Indeed, in rat models of ethanol intoxication, the accumulation of lipid droplets, together with changes in mitochondrial morphology, is first observed in the pericentral zone before spreading into the periportal zone as the disease progresses[108]. This pericentral damage has been hypothesized to be associated with the reactive oxygen species generated by spontaneous fluctuations in blood flow that lead to transient pericentral ischaemia[109]. Similar pericentral zonation patterns were observed in human patients with nonalcoholic or alcoholic fatty liver disease[107,110]. Nevertheless, periportal predominance of fat accumulation has also been observed, for instance, in mice fed methionine and a choline-deficient high-fat diet[111]. In paediatric patients, steatosis is typically azonal or panacinar, whereas pericentral fibrosis zonation is similar to that seen in adults[112].

The liver is a central organ in the progression of malaria infection. The blood-borne *Plasmodium* parasites infect hepatocytes, in which they replicate and develop into merozoites. This liver stage precedes and is necessary for the release of the parasite into the bloodstream, where it commences the pathological stage[113]. Parasite replication has been suggested to be more efficient in pericentral hepatocytes, presumably owing to optimal oxygen tension for liver-stage malaria infection[114]. The distinct cellular states of zonal hepatocytes in terms of oxygen levels, metabolite content and exposure owing to location along the sinusoids suggest that the liver-specific HBVs and HCVs[115,116] might also exhibit zonal hepatocyte infection properties[117].

Autoimmune hepatitis seems to be more common in periportal hepatocytes[118,119]. This zonal preference could be related to an enhanced inflammatory cytokine response brought about by the increased blood flow rate and oxygen consumption in the periportal zone[120]. Another autoimmune-related pathology that manifests predominantly in the portal layers is primary biliary cirrhosis[117]. This chronic disease is characterized by bile duct destruction and portal inflammation, which can lead to cirrhosis and liver failure. At early stages of primary biliary cirrhosis, inflammation with mainly lymphoplasmacytic infiltrates is observed in the portal tract and gives rise to portal bile duct destruction[121,122]. As in autoimmune hepatitis, the increased blood flow in the portal layers might render this zone vulnerable to infiltrating immune cells. The functional heterogeneity of hepatocytes along the lobule radial axis could also translate into differences in the accumulation of mutations and lesions[123–125]. In turn, these differences could result in zonal patterns of oncogenic transformation. The detection of HCC usually occurs at an advanced stage,

Box 2 | Liver zonation in pathological states

Pericentral predominance

- Drugs and compounds
  - Acetominophen[101]
  - Carbon tetrachloride (CCl_4)[103]
  - Ethanol[104]
- Fatty liver disease[107]
- *Plasmodium* parasite infection (malaria)[114]

Periportal predominance

- Drugs and compounds
  - Doxorubicin[102]
  - Galactosamine[105]
  - Allyl alcohol[106]
- Autoimmune hepatitis[118]
- Primary biliary cirrhosis[121]

when tumour size is too large to identify sub-lobular patterns. An outstanding challenge is to characterize the preferential cell of origin for this disease in different HCC aetiologies — be it a pericentral, periportal or mid-zonal hepatocyte[126,127]. BOX 2 summarizes the different susceptibilities of the zones to the various pathologies.

Outlook

Decades of studies into liver zonation have revealed the global transcriptional zonation patterns and key regulatory mechanisms that shape this spatial variability. In this section, we describe some of the future challenges in the field.

Other sources of hepatocyte variability. The patterns of liver zonation described thus far considered a simplified 1D porto-central axis as the sole spatial determinant of hepatocyte molecular identity. In fact, the liver lobule has a more complex 3D polyhedral shape[4,5]. Blood-borne factors or morphogenetic signals flowing or diffusing from the portal nodes can generate variability in hepatocytes that are equidistant from the central vein depending on whether they are close to or far from the lobule corners. Thus, for example, layer 8 hepatocytes (FIG. 3) would consist of a mixture of subpopulations of hepatocytes that might be molecularly distinct depending on their distance from the portal nodes. Similarly, gradients perpendicular to the porto-central lobule plain[128] could generate additional variability. Future spatial reconstructions would uncover the importance of these additional spatial sources of liver heterogeneity.

Another ubiquitous source of liver heterogeneity is hepatocyte polyploidy. Unlike most tissues, in which the majority of cells are mononucleated diploid cells, hepatocytes can have either one or two nuclei, each carrying two, four, eight or even more copies of each chromosome[129,130]. The functional importance of hepatocyte polyploidy is unclear. A tetraploid hepatocyte has twice the volume of a diploid hepatocyte, as well as twice the genetic material, and therefore, if transcriptional regulatory mechanisms were identical between these ploidy classes, cellular mRNA concentrations would also be identical[51]. Alternatively, distinct regulation of genes in hepatocytes of different ploidy classes might yield more optimal liver function. For example, the increased volume to surface area ratio of polyploid hepatocytes might make them more efficient at performing energetically demanding tasks. Notably, hepatocyte polyploidy is also zonated, proceeding more rapidly in the mid-lobule layers than in pericentral or periportal regions as mice age[131,132]. Consequently, teasing out the effect of polyploidy on hepatocyte molecular identity requires the zonation of hepatocytes to be taken into account. Single-cell transcriptomics are well-suited to explore the combined effect of zonation and polyploidy on the hepatocyte cell state[48].

The liver has a remarkable regenerative capacity[133,134]. Although all hepatocytes have the capacity to proliferate upon damage, studies published in the past few years have revealed distinct subpopulations of pericentral[73] or periportal[135–137] hepatocytes that preferentially generate new hepatocytes during homeostasis or regeneration. Exploring the mechanisms that yield hepatocyte regenerative heterogeneity would be critical for cell-based therapy approaches[138].

Interactions between hepatocytes and specific subsets of liver NPCs could yield additional hepatocyte variability. For example, Kupffer cells that encounter bacterial products from the gut release cytokines and other factors that can induce specific gene expression programmes in neighbouring hepatocytes[139]. Single-cell and paired-cell RNA sequencing studies could reveal the molecular circuitries that mediate these and other crosstalk between hepatocytes and zonated NPCs[76].

Zonation of features beyond mRNA. To comprehensively characterize the functional heterogeneity of hepatocytes, it is critical to obtain high-resolution spatial maps for cellular properties other than mRNA, such as DNA methylation patterns, chromosomal conformations and chromatin modifications, proteomes and metabolomes. Although single-cell omics technologies for measuring these features are rapidly advancing[140–144], they still lag behind single-cell transcriptomics in terms of sensitivities.

Alternative approaches to single-cell measurements that can provide information on spatial location for these cellular properties entail the isolation of large populations of cells in a spatially stratified manner, for instance, via LCM[145–147] or fluorescence-activated cell sorting using zonated surface markers. Building on the spatial transcriptomics atlas of the liver, Ben-Moshe et al.[148] utilized the combined expression of the pericentral surface marker CD73 and the periportal surface marker E-cadherin to sort hundreds of thousands of hepatocytes from eight distinct lobule layers. They then used mass spectrometry proteomics[149] and microRNA microarrays to characterize the zonation of hepatocyte proteins and microRNA. This generic approach facilitates a broad range of additional measurements, such as assays for transposase-accessible chromatin sequencing (ATAC-seq)[150], reduced-representation bisulfite sequencing (RRBS)[151] and Hi-C[152,153], thus exposing the spatial variability of these additional features.

In situ technologies such as matrix-assisted laser desorption/ionization (MALDI) mass spectrometry imaging have been used to measure large panels of metabolites[154–156] and revealed zonated patterns of lipid accumulation in mice brains and livers[157–159] and could be applied to investigate the zonation of other liver metabolites. Imaging mass cytometry is another approach for obtaining the protein levels of dozens of genes simultaneously with subcellular spatial resolution[160–162]. Applying these approaches to the liver will provide a deeper understanding of the essence of the hepatocyte cell type and will also be instrumental in constructing computational models of liver metabolic activity[163–165].

Dynamic zonation along physiological processes. The liver is not only spatially heterogeneous; hepatic gene expression also varies over time. The expression of ~25% of liver genes dynamically changes in a circadian manner to match the metabolic requirements of the body[166–170]. These studies on circadian rhythms were

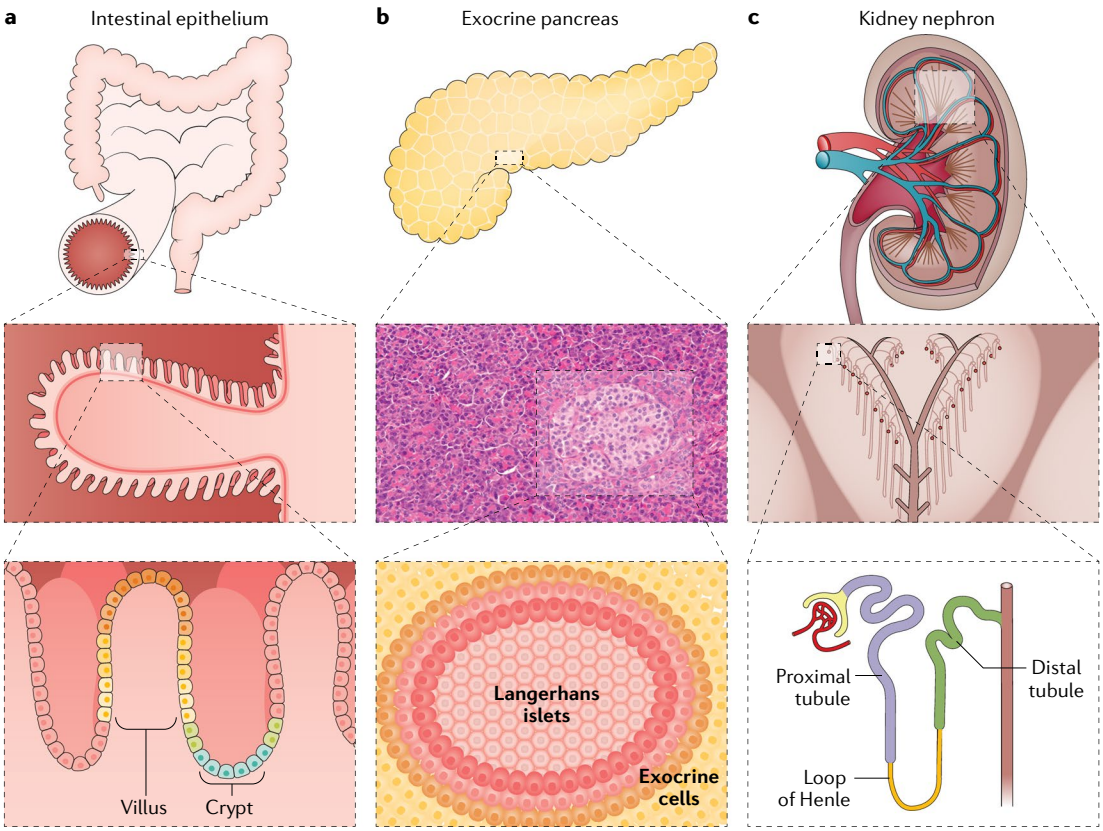

Fig. 6 | **Spatial heterogeneity in other metabolic tissues. a** | The intestinal epithelium is composed of repeating crypt–villus units. Moor at al. uncovered marked zonation of enterocyte gene expression, with more than 80% of the enterocyte genes differentially expressed along the villus axis[146]. Distinct zones along the villus specialize in absorption of distinct nutrients and in immune modulation. **b** | The pancreas consists of acinar cells with exocrine functions and a minority of endocrine cells arranged in the islets of Langerhans. Acinar cells could potentially exhibit zonated gene expression as a function of their distance from the islets. **c** | The kidney nephron is composed of different cell types forming the functional unit of the kidney. Different genes exhibit spatially graded expression along the nephron axis[184–186].

performed using bulk measurements of liver cells and lacked spatial resolution. An open question is whether gene expression in all lobule zones oscillates in a coherent manner, or whether individual zones exhibit circadian oscillations and other zones are less responsive. In addition to circadian rhythms, fasting and feeding also modulate hepatocyte gene expression. To control for this temporal metabolic variability, the spatial transcriptomics study by Bahar Halpern et al.[48] was performed using fasted mice. Similar landmark gene-based spatial reconstruction at different time points around the clock, as well as in fasted or fed mice, could reveal spatiotemporal zonation patterns.

Zonation in the human liver. Most studies on liver zonation have been performed in mice and other rodents. As a consequence, much less is known about spatial heterogeneity in the human liver. Although some genes have been shown to be zonated in humans and rodents alike[147,171], there are also notable differences[60,172–174]. Analysis of the human liver presents several challenges[175]. Unlike model animals that can be sacrificed under a controlled physiological state and in which tissue can be immediately processed, available human liver tissues are generally under non-physiological states. These tissues include samples from deceased donors that have undergone an ischaemic period or from diseased livers obtained during surgery, which often entails xenobiotic exposure. Factors such as these can dramatically modulate liver gene expression[176]. Another challenge for reconstructing zonation maps in humans is the much higher inter-individual variability in liver gene expression than that seen with mice. This variability can be attributed, among other factors, to genetics, sex, age, adiposity and metabolic states. Reconstructing a global high-resolution spatial expression map of the human liver would reveal principles governing division of labour and could expose differential susceptibilities of zonal hepatocytes to a range of pathological perturbations.

Zonation in other tissues. The principle of spatial division of labour for optimizing tissue function is not unique to the liver and seems to be relevant to other metabolic tissues such as the intestine, pancreas and kidney (FIG. 6). The intestinal epithelium consists of repeating crypt–villus units that exhibit gradients of morphogens and oxygen[177], as well as potential spatial gradients of nutrients and bacterial content[178]. Using spatially resolved single-cell transcriptomics, Moor et al. uncovered broad zonation of enterocyte function

along the villus axis, with zonated expression of key nutrient transporters and antibacterial expression programmes[146]. Antimicrobial peptides are specifically produced by enterocytes at the lower villus zones, potentially to create a sterile microenvironment in the adjacent intestinal crypts that harbour the long-lived tissue stem cells. Amino acid and carbohydrate absorption processes, which require cellular ATP, are allocated to the lower-to-mid villus zones, where oxygen concentrations are higher. By contrast, lipids, which can freely diffuse into enterocytes, are preferentially absorbed at the villus tips, a more hypoxic area with less available ATP[146].

The pancreas is another metabolic organ with potential sources of variability. Pancreatic islets, harbouring endocrine cells, are surrounded by exocrine acinar cells. Local signals secreted from the islets might generate zonated gene expression in the surrounding acinar cells[179]. Another tissue in which spatial division of labour might be relevant is the kidney nephron, which essentially possesses a 1D structure with ubiquitous gradients of function. Different cell types are positioned along the nephron axis, and several metabolic processes have been shown to be spatially heterogeneous[18,180–183]. Lee et al.[184] performed deep RNA sequencing of 14 microdissected segments of the rat nephron. This high-throughput method found spatial differential expression of transcription factors and enzymes in the different cell types along the nephron. Single-cell transcriptomics studies have also revealed additional spatial heterogeneity in this structured organ[185,186]. A future challenge will be to develop a theory to explain when spatial division of labour might be more optimal for tissue function[128,187–189].

Conclusions

Hepatocytes exhibit substantial variability in their molecular makeup on the basis of their position along the lobule porto-central axis. This heterogeneity is a result of gradients of oxygen, nutrients, hormones and morphogens, interactions with liver NPCs and potentially zonated intrinsic epigenetic features. Systematically characterizing these layers of heterogeneity will yield a refined definition of the hepatocyte cell type and a better understanding of liver function in health and dysfunction in disease.

Published online: 01 April 2019

1. Jungermann, K. Dynamics of zonal hepatocyte heterogeneity. Perinatal development and adaptive alterations during regeneration after partial hepatectomy, starvation and diabetes. *Acta Histochem. Suppl.* **32**, 89–98 (1986).
2. Gebhardt, R. Metabolic zonation of the liver: regulation and implications for liver function. *Pharmacol. Ther.* **53**, 275–354 (1992).
3. Godoy, P. et al. Recent advances in 2D and 3D in vitro systems using primary hepatocytes, alternative hepatocyte sources and non-parenchymal liver cells and their use in investigating mechanisms of hepatotoxicity, cell signaling and ADME. *Arch. Toxicol.* **87**, 1315–1530 (2013).
4. Hoehme, S. et al. Prediction and validation of cell alignment along microvessels as order principle to restore tissue architecture in liver regeneration. *Proc. Natl Acad. Sci. USA* **107**, 10371–10376 (2010).
5. Teutsch, H. F. The modular microarchitecture of human liver. *Hepatology* **42**, 317–325 (2005).
6. Torre, C., Perret, C. & Colnot, S. Molecular determinants of liver zonation. *Prog. Mol. Biol. Transl Sci.* **97**, 127–150 (2010).
7. Israel, Y. & Orrego, H. Hypermetabolic state and hypoxic liver damage. *Recent Dev. Alcohol.* **2**, 119–133 (1984).
8. Kietzmann, T., Dimova, E. Y., Flügel, D. & Scharf, J.-G. Oxygen: modulator of physiological and pathophysiological processes in the liver. *Z. Gastroenterol.* **44**, 67–76 (2006).
9. de Groot, H., Littauer, A. & Noll, T. in *Oxygen Sensing in Tissues* (ed. Acker, H.) 49–64 (Springer-Verlag Berlin Heidelberg, 1988).
10. Arteel, G. E., Iimuro, Y., Yin, M., Raleigh, J. A. & Thurman, R. G. Chronic enteral ethanol treatment causes hypoxia in rat liver tissue in vivo. *Hepatology* **25**, 920–926 (1997).
11. Matsumura, T. & Thurman, R. G. Measuring rates of O2 uptake in periportal and pericentral regions of liver lobule: stop-flow experiments with perfused liver. *Am. J. Physiol.* **244**, G656–G659 (1983).
12. Jungermann, K. & Keitzmann, T. Zonation of parenchymal and nonparenchymal metabolism in liver. *Annu. Rev. Nutr.* **16**, 179–203 (1996).
13. Jungermann, K. & Katz, N. Functional hepatocellular heterogeneity. *Hepatology* **2**, 385S–395S (1982).
14. Gebhardt, R. & Matz-Soja, M. Liver zonation: novel aspects of its regulation and its impact on homeostasis. *World J. Gastroenterol.* **20**, 8491–8504 (2014).
15. Colnot, S. & Perret, C. in *Molecular Pathology of Liver Diseases* (ed. Monga, S. P. S.) 7–16 (Springer US, 2011).
16. Kater, J. M. Comparative and experimental studies on the cytology of the liver. *Z. Für Zellforsch. Mikrosk. Anat.* **17**, 217–246 (1933).
17. Deane, H. W. A cytological study of the diurnal cycle of the liver of the mouse in relation to storage and secretion. *Anat. Rec.* **88**, 39–65 (1944).
18. Chiquoine, A. D. The distribution of glucose-6-phosphatase in the liver and kidney of the mouse. *J. Histochem. Cytochem.* **1**, 429–435 (1953).
19. Jungermann, K. & Katz, N. Functional specialization of different hepatocyte populations. *Physiol. Rev.* **69**, 708–764 (1989).
20. Jungermann, K., Heilbronn, R., Katz, N. & Sasse, D. The glucose/glucose-6-phosphate cycle in the periportal and perivenous zone of rat liver. *Eur. J. Biochem.* **123**, 429–436 (1982).
21. Andersen, B., Zierz, S. & Jungermann, K. Alteration in zonation of succinate dehydrogenase, phosphoenolpyruvate carboxykinase and glucose-6-phosphatase in regenerating rat liver. *Histochemistry* **80**, 97–101 (1984).
22. Nauck, M., Wölfle, D., Katz, N. & Jungermann, K. Modulation of the glucagon-dependent induction of phosphoenolpyruvate carboxykinase and tyrosine aminotransferase by arterial and venous oxygen concentrations in hepatocyte cultures. *Eur. J. Biochem.* **119**, 657–661 (1981).
23. Sasse, D., Katz, N. & Jungermann, K. Functional heterogeneity of rat liver parenchyma and of isolated hepatocytes. *FEBS Lett.* **57**, 83–88 (1975).
24. Feldmann, G., Scoazec, J. Y., Racine, L. & Bernuau, D. Functional hepatocellular heterogeneity for the production of plasma proteins. *Enzyme* **46**, 139–154 (1992).
25. Quistorff, B., Grunnet, N. & Cornell, N. W. Digitonin perfusion of rat liver. A new approach in the study of intra-acinar and intracellular compartmentation in the liver. *Biochem. J.* **226**, 289–297 (1985).
26. Quistorff, B. & Grunnet, N. Dual-digitonin-pulse perfusion. Concurrent sampling of periportal and perivenous cytosol of rat liver for determination of metabolites and enzyme activities. *Biochem. J.* **243**, 87–95 (1987).
27. Gebhardt, R. in *Cytochrome P450 Protocols* (eds Phillips, I. R. & Shephard, E. A.) 319–328 (Humana Press, 1998).
28. Lindros, K. O. & Penttilä, K. E. Digitonin-collagenase perfusion for efficient separation of periportal or perivenous hepatocytes. *Biochem. J.* **228**, 757–760 (1985).
29. Racine, L. et al. Distribution of albumin, α1-inhibitor 3 and their respective mRNAs in periportal and perivenous rat hepatocytes isolated by the digitonin-collagenase technique. *Biochem. J.* **305**, 263–268 (1995).
30. Braeuning, A. et al. Differential gene expression in periportal and perivenous mouse hepatocytes. *FEBS J.* **273**, 5051–5061 (2006).
31. Saito, K., Negishi, M. & Squires, E. J. Sexual dimorphisms in zonal gene expression in mouse liver. *Biochem. Biophys. Res. Commun.* **436**, 730–735 (2013).
32. Hashimshony, T., Wagner, F., Sher, N. & Yanai, I. CEL-Seq: single-cell RNA-Seq by multiplexed linear amplification. *Cell Rep.* **2**, 666–673 (2012).
33. Jaitin, D. A. et al. Massively parallel single cell RNA-Seq for marker-free decomposition of tissues into cell types. *Science* **343**, 776 (2014).
34. Zeisel, A. et al. Cell types in the mouse cortex and hippocampus revealed by single-cell RNA-seq. *Science* **347**, 1138–1142 (2015).
35. Klein, A. M. et al. Droplet barcoding for single-cell transcriptomics applied to embryonic stem cells. *Cell* **161**, 1187–1201 (2015).
36. Macosko, E. Z. et al. Highly parallel genome-wide expression profiling of individual cells using nanoliter droplets. *Cell* **161**, 1202–1214 (2015).
37. Kolodziejczyk, A. A., Kim, J. K., Svensson, V., Marioni, J. C. & Teichmann, S. A. The technology and biology of single-cell RNA sequencing. *Mol. Cell* **58**, 610–620 (2015).
38. Fu, G. K., Hu, J., Wang, P.-H. & Fodor, S. P. A. Counting individual DNA molecules by the stochastic attachment of diverse labels. *Proc. Natl Acad. Sci. USA* **108**, 9026–9031 (2011).
39. Kivioja, T. et al. Counting absolute numbers of molecules using unique molecular identifiers. *Nat. Methods* **9**, 72 (2012).
40. Casbon, J. A., Osborne, R. J., Brenner, S. & Lichtenstein, C. P. A method for counting PCR template molecules with application to next-generation sequencing. *Nucleic Acids Res.* **39**, e81 (2011).
41. Shiroguchi, K., Jia, T. Z., Sims, P. A. & Xie, X. S. Digital RNA sequencing minimizes sequence-dependent bias and amplification noise with optimized single-molecule barcodes. *Proc. Natl Acad. Sci. USA* **109**, 1347–1352 (2012).
42. Islam, S. et al. Characterization of the single-cell transcriptional landscape by highly multiplex RNA-seq. *Genome Res.* **21**, 1160–1167 (2011).
43. Marinov, G. K. et al. From single-cell to cell-pool transcriptomes: stochasticity in gene expression and RNA splicing. *Genome Res.* **24**, 496–510 (2014).
44. Satija, R., Farrell, J. A., Gennert, D., Schier, A. F. & Regev, A. Spatial reconstruction of single-cell gene expression data. *Nat. Biotechnol.* **33**, 495–502 (2015).
45. Achim, K. et al. High-throughput spatial mapping of single-cell RNA-seq data to tissue of origin. *Nat. Biotechnol.* **33**, 503–509 (2015).
46. Itzkovitz, S. & van Oudenaarden, A. Validating transcripts with probes and imaging technology. *Nat. Methods* **8**, S12 (2011).

47. Raj, A., van den Bogaard, P., Rifkin, S. A., van Oudenaarden, A. & Tyagi, S. Imaging individual mRNA molecules using multiple singly labeled probes. *Nat. Methods* **5**, 877 (2008).
48. Bahar Halpern, K. et al. Single-cell spatial reconstruction reveals global division of labour in the mammalian liver. *Nature* **542**, 352–356 (2017).
49. Stouthamer, A. H. A theoretical study on the amount of ATP required for synthesis of microbial cell material. *Antonie Van Leeuwenhoek* **39**, 545–565 (1973).
50. Rolfe, D. F. & Brown, G. C. Cellular energy utilization and molecular origin of standard metabolic rate in mammals. *Physiol. Rev.* **77**, 731–758 (1997).
51. Bahar Halpern, K. et al. Bursty gene expression in the intact mammalian liver. *Mol. Cell* **58**, 147–156 (2015).
52. Rappaport, A. M., Borowy, Z. J., Lougheed, W. M. & Lotto, W. N. Subdivision of hexagonal liver lobules into a structural and functional unit. Role in hepatic physiology and pathology. *Anat. Rec.* **119**, 11–33 (1954).
53. Truksa, J., Lee, P. & Beutler, E. The role of STAT, AP-1, E-box and TIEG motifs in the regulation of hepcidin by IL-6 and BMP-9: lessons from human HAMP and murine Hamp1 and Hamp2 gene promoters. *Blood Cells Mol. Dis.* **39**, 255–262 (2007).
54. de Aguiar Vallim, T. Q., Tarling, E. J. & Edwards, P. A. Pleiotropic roles of bile acids in metabolism. *Cell Metab.* **17**, 657–669 (2013).
55. Russell, D. W. The enzymes, regulation, and genetics of bile acid synthesis. *Annu. Rev. Biochem.* **72**, 137–174 (2003).
56. Dawson, P. A. in *Physiology of the Gastrointestinal Tract* (ed. Said, H.) 6th edn 931–956 (Academic Press, 2018).
57. Berndt, N., Horger, M. S., Bulik, S. & Holzhütter, H.-G. A multiscale modelling approach to assess the impact of metabolic zonation and microperfusion on the hepatic carbohydrate metabolism. *PLOS Comput. Biol.* **14**, e1006005 (2018).
58. Katz, N., Teutsch, H. F., Jungermann, K. & Sasse, D. Heterogeneous reciprocal localization of fructose-1, 6-bis-phosphatase and of glucokinase in microdissected periportal and perivenous rat liver tissue. *FEBS Lett.* **83**, 272–276 (1977).
59. Häussinger, D. Hepatocyte heterogeneity in glutamine and ammonia metabolism and the role of an intercellular glutamine cycle during ureogenesis in perfused rat liver. *Eur. J. Biochem.* **133**, 269–275 (1983).
60. Haüssinger, D. Nitrogen metabolism in liver: structural and functional organization and physiological relevance. *Biochem. J.* **267**, 281 (1990).
61. Gebhardt, R. & Mecke, D. Heterogeneous distribution of glutamine synthetase among rat liver parenchymal cells in situ and in primary culture. *EMBO J.* **2**, 567–570 (1983).
62. Schliess, F. et al. Integrated metabolic spatial-temporal model for the prediction of ammonia detoxification during liver damage and regeneration. *Hepatology* **60**, 2040–2051 (2014).
63. Bartl, M. et al. Optimality in the zonation of ammonia detoxification in rodent liver. *Arch. Toxicol.* **89**, 2069–2078 (2015).
64. Häussinger, D. Glutamine metabolism in the liver: overview and current concepts. *Metabolism* **38**, 14–17 (1989).
65. Schleicher, J. et al. Zonation of hepatic fatty acid metabolism — the diversity of its regulation and the benefit of modeling. *Biochim. Biophys. Acta* **1851**, 641–656 (2015).
66. Bar-Even, A. et al. The moderately efficient enzyme: evolutionary and physicochemical trends shaping enzyme parameters. *Biochemistry* **50**, 4402–4410 (2011).
67. Lieburg-Apers, D. C. et al. Quantitative glucose and ATP sensing in mammalian cells. *Pharm. Res.* **28**, 2745–2757 (2011).
68. Hakvoort, T. B. M. et al. Pivotal role of glutamine synthetase in ammonia detoxification. *Hepatology* **65**, 281–293 (2017).
69. Augustin, H. G. & Koh, G. Y. Organotypic vasculature: from descriptive heterogeneity to functional pathophysiology. *Science* **357**, eaal2379 (2017).
70. Aird, W. C. Phenotypic heterogeneity of the endothelium: II. Representative vascular beds. *Circ. Res.* **100**, 174–190 (2007).
71. Strauss, O., Phillips, A., Ruggiero, K., Bartlett, A. & Dunbar, P. R. Immunofluorescence identifies distinct subsets of endothelial cells in the human liver. *Sci. Rep.* **7**, 44356 (2017).
72. Rafii, S., Butler, J. M. & Ding, B.-S. Angiocrine functions of organ-specific endothelial cells. *Nature* **529**, 316 (2016).
73. Wang, B., Zhao, L., Fish, M., Logan, C. Y. & Nusse, R. Self-renewing diploid Axin2$^+$ cells fuel homeostatic renewal of the liver. *Nature* **524**, 180–185 (2015).
74. Carmon, K. S., Gong, X., Lin, Q., Thomas, A. & Liu, Q. R-Spondins function as ligands of the orphan receptors LGR4 and LGR5 to regulate Wnt/β-catenin signaling. *Proc. Natl Acad. Sci. USA* **108**, 11452–11457 (2011).
75. Planas-Paz, L. et al. The RSPO–LGR4/5–ZNRF3/RNF43 module controls liver zonation and size. *Nat. Cell Biol.* **18**, 467 (2016).
76. Halpern, K. et al. Paired-cell sequencing enables spatial gene expression mapping of liver endothelial cells. *Nat. Biotechnol.* **36**, 962–970 (2018).
77. Bykov, I., Ylipaasto, P., Eerola, L. & Lindros, K. O. Functional differences between periportal and perivenous kupffer cells isolated by digitonin-collagenase perfusion. *Comp. Hepatol.* **3**, S34 (2004).
78. Friedman, S. L. Hepatic stellate cells: protean, multifunctional, and enigmatic cells of the liver. *Physiol. Rev.* **88**, 125–172 (2008).
79. Friedman, S. L. Molecular regulation of hepatic fibrosis, an integrated cellular response to tissue injury. *J. Biol. Chem.* **275**, 2247–2250 (2000).
80. Preziosi, M., Okabe, H., Poddar, M., Singh, S. & Monga, S. P. Endothelial Wnts regulate β-catenin signaling in murine liver zonation and regeneration: a sequel to the Wnt–Wnt situation. *Hepatol. Commun.* **2**, 845 (2018).
81. Burke, Z. D. & Tosh, D. The Wnt/β-catenin pathway: master regulator of liver zonation? *Bioessays* **28**, 1072–1077 (2006).
82. Thompson, M. D. & Monga, S. P. S. WNT/β-catenin signaling in liver health and disease. *Hepatology* **45**, 1298–1305 (2007).
83. Benhamouche, S. et al. Apc tumor suppressor gene is the 'zonation-keeper' of mouse liver. *Dev. Cell* **10**, 759–770 (2006).
84. Sekine, S., Lan, B. Y.-A., Bedolli, M., Feng, S. & Hebrok, M. Liver-specific loss of β-catenin blocks glutamine synthesis pathway activity and cytochrome p450 expression in mice. *Hepatology* **43**, 817–825 (2006).
85. Rocha, A. S. et al. The angiocrine factor Rspondin3 is a key determinant of liver zonation. *Cell Rep.* **13**, 1757–1764 (2015).
86. Matz-Soja, M. et al. Hedgehog signaling is a potent regulator of liver lipid metabolism and reveals a GLI-code associated with steatosis. *eLife* **5**, e13308 (2016).
87. Wölfle, D., Schmidt, H. & Jungermann, K. Short-term modulation of glycogen metabolism, glycolysis and gluconeogenesis by physiological oxygen concentrations in hepatocyte cultures. *Eur. J. Biochem.* **135**, 405–412 (2005).
88. Jungermann, K. & Kietzmann, T. Role of oxygen in the zonation of carbohydrate metabolism and gene expression in liver. *Kidney Int.* **51**, 402–412 (1997).
89. Kietzmann, T. Metabolic zonation of the liver: the oxygen gradient revisited. *Redox Biol.* **11**, 622–630 (2017).
90. Kaidi, A., Williams, A. C. & Paraskeva, C. Interaction between β-catenin and HIF-1 promotes cellular adaptation to hypoxia. *Nat. Cell Biol.* **9**, 210 (2007).
91. Lehwald, N. et al. Wnt–β-catenin signaling protects against hepatic ischemia and reperfusion injury in mice. *Gastroenterology* **141**, 707–718 (2011).
92. Cheng, X. et al. Glucagon contributes to liver zonation. *Proc. Natl Acad. Sci. USA* **115**, E4111–E4119 (2018).
93. Waxman, D. J. & Chang, T. K. H. in *Cytochrome P450: Structure, Mechanism, and Biology* (ed. Ortiz de Montellano, P. R.) 2nd edn 391–417 (Springer US, 1995).
94. Oinonen, T. & Lindros, K. O. Zonation of hepatic cytochrome P-450 expression and regulation. *Biochem. J.* **329**, 17–35 (1998).
95. Bird, A. DNA methylation patterns and epigenetic memory. *Genes Dev.* **16**, 6–21 (2002).
96. Kaplan, S., Bren, A., Zaslaver, A., Dekel, E. & Alon, U. Diverse two-dimensional input functions control bacterial sugar genes. *Mol. Cell* **29**, 786–792 (2008).
97. Brosch, M. et al. Epigenomic map of human liver reveals principles of zonated morphogenic and metabolic control. *Nat. Commun.* **9**, 4150 (2018).
98. Tujios, S. & Fontana, R. J. Mechanisms of drug-induced liver injury: from bedside to bench. *Nat. Rev. Gastroenterol. Hepatol.* **8**, 202 (2011).
99. Nelson, S. D. Molecular mechanisms of the hepatotoxicity caused by acetaminophen. *Semin. Liver Dis.* **10**, 267–278 (1990).
100. Makin, A. J., Wendon, J. & Williams, R. A. 7-year experience of severe acetaminophen-induced hepatotoxicity (1987–1993). *Gastroenterology* **109**, 1907–1916 (1995).
101. Anundi, I., Lähteenmäki, T., Rundgren, M., Moldeus, P. & Lindros, K. O. Zonation of acetaminophen metabolism and cytochrome P450 2E1-mediated toxicity studied in isolated periportal and perivenous hepatocytes. *Biochem. Pharmacol.* **45**, 1251–1259 (1993).
102. Ganey, P. E., Kauffman, F. C. & Thurman, R. G. Oxygen-dependent hepatotoxicity due to doxorubicin: role of reducing equivalent supply in perfused rat liver. *Mol. Pharmacol.* **34**, 695–701 (1988).
103. Badger, D. A., Sauer, J. M., Hoglen, N. C., Jolley, C. S. & Sipes, I. G. The role of inflammatory cells and cytochrome P450 in the potentiation of CCl4-induced liver injury by a single dose of retinol. *Toxicol. Appl. Pharmacol.* **141**, 507–519 (1996).
104. Keegan, A., Martini, R. & Batey, R. Ethanol-related liver injury in the rat: a model of steatosis, inflammation and pericentral fibrosis. *J. Hepatol.* **23**, 591–600 (1995).
105. Zieve, L., Anderson, W. R. & Dozeman, R. Hepatic regenerative enzyme activity after diffuse injury with galactosamine: relationship to histologic alterations. *J. Lab. Clin. Med.* **112**, 575–582 (1988).
106. Reid, W. D. Mechanism of allyl alcohol-induced hepatic necrosis. *Experientia* **28**, 1058–1061 (1972).
107. Brunt, E. M. Pathology of fatty liver disease. *Mod. Pathol.* **20**, S40 (2007).
108. Iseri, O. A., Lieber, C. S. & Gottlieb, L. S. The ultrastructure of fatty liver induced by prolonged ethanol ingestion. *Am. J. Pathol.* **48**, 535–555 (1966).
109. Farrell, G. C., Teoh, N. C. & Mccuskey, R. S. Hepatic microcirculation in fatty liver disease. *Anat. Rec.* **291**, 684–692 (2008).
110. Chalasani, N. et al. Relationship of steatosis grade and zonal location to histological features of steatohepatitis in adult patients with non-alcoholic fatty liver disease. *J. Hepatol.* **48**, 829 (2008).
111. Schwen, L. O. et al. Zonated quantification of steatosis in an entire mouse liver. *Comput. Biol. Med.* **73**, 108–118 (2016).
112. Hijmans, B. S., Grefhorst, A., Oosterveer, M. H. & Groen, A. K. Zonation of glucose and fatty acid metabolism in the liver: mechanism and metabolic consequences. *Biochimie* **96**, 121–129 (2014).
113. Prudêncio, M., Rodriguez, A. & Mota, M. M. The silent path to thousands of merozoites: the *Plasmodium* liver stage. *Nat. Rev. Microbiol.* **4**, 849 (2006).
114. Ng, S. et al. Hypoxia promotes liver stage malaria infection in primary human hepatocytes in vitro. *Dis. Model. Mech.* **7**, 215–224 (2013).
115. Seeger, C. & Mason, W. S. Hepatitis B virus biology. *Microbiol. Mol. Biol. Rev.* **64**, 51–68 (2000).
116. Chisari, F. V. Unscrambling hepatitis C virus–host interactions. *Nature* **436**, 930–932 (2005).
117. Bedossa, P., Dargère, D. & Paradis, V. Sampling variability of liver fibrosis in chronic hepatitis C. *Hepatology* **38**, 1449–1457 (2003).
118. Diamantis, I. & Boumpas, D. T. Autoimmune hepatitis: evolving concepts. *Autoimmun. Rev.* **3**, 207–214 (2004).
119. Lohse, A. W., Manns, M., Dienes, H.-P., Büschenfelde, K.-H. M. Z. & Cohen, I. R. Experimental autoimmune hepatitis: disease induction, time course and T-cell reactivity. *Hepatology* **11**, 24–30 (2005).
120. Lettmann, K. A. & Hardtke-Wolenski, M. The importance of liver microcirculation in promoting autoimmune hepatitis via maintaining an inflammatory cytokine milieu – a mathematical model study. *J. Theor. Biol.* **348**, 33–46 (2014).
121. Nakamura, M. et al. Anti-gp210 and anti-centromere antibodies are different risk factors for the progression of primary biliary cirrhosis. *Hepatology* **45**, 118–127 (2007).
122. Selmi, C., Coppel, R. L. & Gershwin, M. E. in *The Autoimmune Diseases* (eds Mackay, I. R. & Rose, N. R.) 4th edn 749–765 (Academic Press, 2006).
123. Llovet, J. M. et al. Hepatocellular carcinoma. *Nat. Rev. Dis. Primers* **2**, 16018 (2016).
124. Nault, J. C. et al. High frequency of telomerase reverse-transcriptase promoter somatic mutations in hepatocellular carcinoma and preneoplastic lesions. *Nat. Commun.* **4**, 2218 (2013).
125. Zucman-Rossi, J., Villanueva, A., Nault, J. C. & Llovet, J. M. Genetic landscape and biomarkers of hepatocellular carcinoma. *Gastroenterology* **149**, 1226–1239 (2015).
126. Sia, D., Villanueva, A., Friedman, S. L. & Llovet, J. M. Liver cancer cell of origin, molecular class, and effects

on patient prognosis. *Gastroenterology* **152**, 745–761 (2017).
127. Vaupel, P., Kallinowski, F. & Okunieff, P. Blood flow, oxygen and nutrient supply, and metabolic microenvironment of human tumors: a review. *Cancer Res.* **49**, 6449–6465 (1989).
128. Adler, M., Kohanim, Y. K., Tendler, A., Mayo, A. & Alon, U. Continuum of gene-expression profiles provides spatial division of labor within a differentiated cell type. *Cell Syst.* **8**, 43–52 (2019).
129. Celton-Morizur, S. & Desdouets, C. Polyploidization of liver cells. *Adv. Exp. Med. Biol.* **676**, 123–135 (2010).
130. Duncan, A. W. Aneuploidy, polyploidy and ploidy reversal in the liver. *Semin. Cell Dev. Biol.* **24**, 347–356 (2013).
131. Tanami, S. et al. Dynamic zonation of liver polyploidy. *Cell Tissue Res.* **368**, 405–410 (2017).
132. Morales-Navarrete, H. et al. A versatile pipeline for the multi-scale digital reconstruction and quantitative analysis of 3D tissue architecture. *eLife* **4**, e11214 (2015).
133. Yanger, K. & Stanger, B. Z. Facultative stem cells in liver and pancreas: fact and fancy. *Dev. Dyn.* **240**, 521–529 (2011).
134. Michalopoulos, G. K. & DeFrances, M. C. Liver regeneration. *Science* **276**, 60–66 (1997).
135. Alwahsh, S. M., Rashidi, H. & Hay, D. C. Liver cell therapy: is this the end of the beginning? *Cell. Mol. Life Sci.* **75**, 1307–1324 (2018).
136. Tarlow, B. D. et al. Bipotential adult liver progenitors are derived from chronically injured mature hepatocytes. *Cell Stem Cell* **15**, 605–618 (2014).
137. Font-Burgada, J. et al. Hybrid periportal hepatocytes regenerate the injured liver without giving rise to cancer. *Cell* **162**, 766–779 (2015).
138. Forbes, S. J., Gupta, S. & Dhawan, A. Cell therapy for liver disease: from liver transplantation to cell factory. *J. Hepatol.* **62**, S157–S169 (2015).
139. Bilzer, M., Roggel, F. & Gerbes, A. L. Role of Kupffer cells in host defense and liver disease. *Liver Int.* **26**, 1175–1186 (2006).
140. Kelsey, G., Stegle, O. & Reik, W. Single-cell epigenomics: recording the past and predicting the future. *Science* **358**, 69–75 (2017).
141. Buenrostro, J. D. et al. Single-cell chromatin accessibility reveals principles of regulatory variation. *Nature* **523**, 486 (2015).
142. Furlan-Magaril, M., Várnai, C., Nagano, T. & Fraser, P. 3D genome architecture from populations to single cells. *Curr. Opin. Genet. Dev.* **31**, 36–41 (2015).
143. Budnik, B., Levy, E., Harmange, G. & Slavov, N. SCoPE-MS: mass spectrometry of single mammalian cells quantifies proteome heterogeneity during cell differentiation. *Genome Biol.* **19**, 161 (2018).
144. Cusanovich, D. A. et al. A single-cell atlas of in vivo mammalian chromatin accessibility. *Cell* **174**, 1309–1324 (2018).
145. Moor, A. E. et al. Global mRNA polarization regulates translation efficiency in the intestinal epithelium. *Science* **357**, 1299–1303 (2017).
146. Moor, A. E. et al. Spatial reconstruction of single enterocytes uncovers broad zonation along the intestinal villus axis. *Cell* **175**, 1156–1167 (2018).
147. McEnerney, L. et al. Dual modulation of human hepatic zonation via canonical and non-canonical Wnt pathways. *Exp. Mol. Med.* **49**, e413 (2017).
148. Ben-Moshe, S., Shapira, Y., Moor, A. E., Halpern, K. B. & Itzkovitz, S. Spatial sorting enables comprehensive characterization of liver zonation. *Preprint at bioRxiv* https://doi.org/10.1101/529784 (2019).
149. Aebersold, R. & Mann, M. Mass spectrometry-based proteomics. *Nature* **422**, 198–207 (2003).
150. Buenrostro, J. D., Wu, B., Chang, H. Y. & Greenleaf, W. J. ATAC-seq: a method for assaying chromatin accessibility genome-wide. *Curr. Protoc. Mol. Biol.* **109**, 21.29.1–21.29.9 (2015).
151. Meissner, A. et al. Reduced representation bisulfite sequencing for comparative high-resolution DNA methylation analysis. *Nucleic Acids Res.* **33**, 5868–5877 (2005).
152. Dixon, J. R. et al. Topological domains in mammalian genomes identified by analysis of chromatin interactions. *Nature* **485**, 376 (2012).
153. Lieberman-Aiden, E. et al. Comprehensive mapping of long-range interactions reveals folding principles of the human genome. *Science* **326**, 289–293 (2009).
154. Caprioli, R. M., Farmer, T. B. & Gile, J. Molecular imaging of biological samples: localization of peptides and proteins using MALDI-TOF MS. *Anal. Chem.* **69**, 4751–4760 (1997).
155. Cornett, D. S., Reyzer, M. L., Chaurand, P. & Caprioli, R. M. MALDI imaging mass spectrometry: molecular snapshots of biochemical systems. *Nat. Methods* **4**, 828 (2007).
156. Stoeckli, M., Staab, D. & Schweitzer, A. Compound and metabolite distribution measured by MALDI mass spectrometric imaging in whole-body tissue sections. *Int. J. Mass Spectrom.* **260**, 195–202 (2007).
157. Shrivas, K. et al. Ionic matrix for enhanced MALDI imaging mass spectrometry for identification of phospholipids in mouse liver and cerebellum tissue sections. *Anal. Chem.* **82**, 8800–8806 (2010).
158. Shimma, S. et al. MALDI-based imaging mass spectrometry revealed abnormal distribution of phospholipids in colon cancer liver metastasis. *J. Chromatogr. B Analyt. Technol. Biomed. Life Sci.* **855**, 98–103 (2007).
159. Chaurand, P., Cornett, D. S., Angel, P. M. & Caprioli, R. M. From whole-body sections down to cellular level, multiscale imaging of phospholipids by MALDI mass spectrometry. *Mol. Cell. Proteomics* **10**, O110.004259 (2011).
160. Angelo, M. et al. Multiplexed ion beam imaging of human breast tumors. *Nat. Med.* **20**, 436 (2014).
161. Bodenmiller, B. Multiplexed epitope-based tissue imaging for discovery and healthcare applications. *Cell Syst.* **2**, 225–238 (2016).
162. Chang, Q. et al. Imaging mass cytometry. *Cytometry A* **91**, 160–169 (2017).
163. Holzhütter, H.-G. The principle of flux minimization and its application to estimate stationary fluxes in metabolic networks. *Eur. J. Biochem.* **271**, 2905–2922 (2004).
164. Holzhütter, H.-G., Drasdo, D., Preusser, T., Lippert, J. & Henney, A. M. The virtual liver: a multidisciplinary, multilevel challenge for systems biology. *Wiley Interdiscip. Rev. Syst. Biol. Med.* **4**, 221–235 (2012).
165. Ricken, T. et al. Modeling function–perfusion behavior in liver lobules including tissue, blood, glucose, lactate and glycogen by use of a coupled two-scale PDE–ODE approach. *Biomech. Model. Mechanobiol.* **14**, 515–536 (2015).
166. Atger, F. et al. Circadian and feeding rhythms differentially affect rhythmic mRNA transcription and translation in mouse liver. *Proc. Natl Acad. Sci. USA* **112**, E6579–E6588 (2015).
167. Mauvoisin, D. et al. Circadian clock-dependent and -independent rhythmic proteomes implement distinct diurnal functions in mouse liver. *Proc. Natl Acad. Sci. USA* **111**, 167–172 (2014).
168. Robles, M. S., Cox, J. & Mann, M. In-vivo quantitative proteomics reveals a key contribution of post-transcriptional mechanisms to the circadian regulation of liver metabolism. *PLOS Genet.* **10**, e1004047 (2014).
169. Storch, K.-F. et al. Extensive and divergent circadian gene expression in liver and heart. *Nature* **417**, 78–83 (2002).
170. Akhtar, R. A. et al. Circadian cycling of the mouse liver transcriptome, as revealed by cDNA microarray, is driven by the suprachiasmatic nucleus. *Curr. Biol.* **12**, 540–550 (2002).
171. Moorman, A. F. M., Vermeulen, J. L. M., Charles, R. & Lamers, W. H. Localization of ammonia-metabolizing enzymes in human liver: ontogenesis of heterogeneity. *Hepatology* **9**, 367–372 (2005).
172. Dingemanse, M. A. et al. Development of the ornithine cycle in rat liver: zonation of a metabolic pathway. *Hepatology* **24**, 407–411 (1996).
173. Agius, L. & Tosh, D. Acinar zonation of cytosolic but not organelle-bound activities of phosphoenolpyruvate carboxykinase and aspartate aminotransferase in guinea-pig liver. *Biochem. J.* **271**, 387–391 (1990).
174. Wimmer, M., Luttringer, C. & Colombi, M. Enzyme activity patterns of phosphoenolpyruvate carboxykinase, pyruvate kinase, glucose-6-phosphate-dehydrogenase and malic enzyme in human liver. *Histochemistry* **93**, 409–415 (1990).
175. MacParland, S. A. et al. Single cell RNA sequencing of human liver reveals distinct intrahepatic macrophage populations. *Nat. Commun.* **9**, 4383 (2018).
176. Chen, M. et al. Drug-induced liver injury: Interactions between drug properties and host factors. *J. Hepatol.* **63**, 503–514 (2015).
177. Albenberg, L. et al. Correlation between intraluminal oxygen gradient and radial partitioning of intestinal microbiota. *Gastroenterology* **147**, 1055–1063 (2014).
178. Belzer, C. & de Vos, W. M. Microbes inside—from diversity to function: the case of Akkermansia. *ISME J.* **6**, 1449–1458 (2012).
179. White, J. W. & Swartz, F. J. Changes in polyploidization of exocrine pancreas in db/db diabetic and normal mice. *Eur. J. Endocrinol.* **94**, 523–528 (1980).
180. Lawrence, G. M., Jepson, M. A., Trayer, I. P. & Walker, D. G. The compartmentation of glycolytic and gluconeogenic enzymes in rat kidney and liver and its significance to renal and hepatic metabolism. *Histochem. J.* **18**, 45–53 (1986).
181. Schmidt, U. & Guder, W. G. Sites of enzyme activity along the nephron. *Kidney Int.* **9**, 233–242 (1976).
182. Burch, H. B. et al. Distribution along the rat nephron of three enzymes of gluconeogenesis in acidosis and starvation. *Am. J. Physiol.* **235**, F246–F253 (1978).
183. Guder, W. G. & Ross, B. D. Enzyme distribution along the nephron. *Kidney Int.* **26**, 101–111 (1984).
184. Lee, J. W., Chou, C.-L. & Knepper, M. A. Deep sequencing in microdissected renal tubules identifies nephron segment–specific transcriptomes. *J. Am. Soc. Nephrol.* **26**, 2669–2677 (2015).
185. Der, E. et al. Single cell RNA sequencing to dissect the molecular heterogeneity in lupus nephritis. *JCI Insight* **2**, 93009 (2017).
186. Park, J. et al. Single-cell transcriptomics of the mouse kidney reveals potential cellular targets of kidney disease. *Science* **360**, 758–763 (2018).
187. Shoval, O. et al. Evolutionary trade-offs, Pareto optimality, and the geometry of phenotype space. *Science* **336**, 1157–1160 (2012).
188. Hart, Y. et al. Inferring biological tasks using Pareto analysis of high-dimensional data. *Nat. Methods* **12**, 233 (2015).
189. Nagrath, D. et al. Integrated energy and flux balance based multiobjective framework for large-scale metabolic networks. *Ann. Biomed. Eng.* **35**, 863–885 (2007).
190. Grün, D. & van Oudenaarden, A. Design and analysis of single-cell sequencing experiments. *Cell* **163**, 799–810 (2015).

Acknowledgements
The authors thank K. Bahar Halpern, Y. Shapira and A. Afriat for valuable comments. S.I. is supported by the Henry Chanoch Krenter Institute for Biomedical Imaging and Genomics, the Leir Charitable Foundations, the Richard Jakubskind Laboratory of Systems Biology, the Cymerman-Jakubskind Prize, the Lord Sieff of Brimpton Memorial Fund, the I-CORE programme of the Planning and Budgeting Committee and the Israel Science Foundation (grants 1902/12 and 1796/12), Israel Science Foundation grant number 1486/16, the European Molecular Biology Organization (EMBO) Young Investigator Program, the European Research Council (ERC) under the European Union's Seventh Framework Programme (FP7/2007-2013 and ERC grant agreement number 335122), the European Research Council (ERC) under the European Union's Horizon 2020 research and innovation programme (grant agreement number 768956), the Bert L. and N. Kuggie Vallee Foundation and the Howard Hughes Medical Institute (HHMI) international research scholar award.

Author contributions
Both authors contributed equally to this Review.

Competing interests
The authors declare no competing interests.

Reviewer information
Nature Reviews Gastroenterology & Hepatology thanks S. Colnot, R. Gebhart and the other anonymous reviewer(s), for their contribution to the peer review of this work.